UNIVERSITY OF SOUTH BOHEMIA IN ČESKÉ BUDĚJOVICE
FACULTY OF SCIENCE

Crystallization and structure-functional studies of bacterial haloalkane dehalogenases and His phosphotransfer protein AHP2 from model plant *A. thaliana*

Ph.D. THESIS

Oksana Degtjarik, MSc

Supervisor: Doc. Mgr. Ivana Kuta Smatanova, Ph.D.
University of South Bohemia in České Budějovice, Faculty of Science

České Budějovice 2014

This thesis should be cited as:

Degtjarik O., 2014: Crystallization and structure-functional studies of bacterial haloalkane dehalogenases and His phosphotransfer protein AHP2 from model plant *A. thaliana*. Ph.D. Thesis. Series, No. 12. University of South Bohemia, Faculty of Science, České Budějovice, Czech Republic, 159 pp.

Annotation

X-ray crystallography is the most powerful experimental technique for studying three-dimensional structure of proteins. Knowledge the protein structure allows us to understand different biological processes, such as mechanisms of enzymatic reactions and protein-protein interactions, at their basic level. Haloalkane dehalogenase LinB was chosen for this study as an enzyme able to convert a large group of environmental pollutants. Due to its broad substrate specificity, LinB can be potentially applied for bioremediation of xenobiotic compounds. On the other side, studying of histidine-phosphotransfer protein AHP2 structure allows us to get insights into structural determinants of interaction specificity within multistep signaling system in *A. thaliana.*

This thesis consists of two main parts. The first part is focused on crystallization and structural analysis of newly prepared haloalkane dehalogenase (HLD) LinB mutant variants LinB32 and LinB86 in order to explore the effect of mutations on enzyme functionality from structural point of view. Additionally, the crystallization and preliminary X-ray diffraction analysis of LinB HLD mutant LinB70 with introduced the second halide-binding site from DbeA enzyme is reported.

The second part of the thesis describes the crystallization and structure-functional analysis of histidine-phosphotransfer protein AHP2 from *Arabidopsis thaliana*. The structural features potentially responsible for the specificity of interaction between AHP2 and histidine kinase CKI1 within *Arabidopsis* multistep signaling pathway were investigated by means of molecular dynamics simulations.

.

Declaration [in Czech]

Prohlašuji, že svoji disertační práci jsem vypracovala samostatně pouze s použitím pramenů a literatury uvedených v seznamu citované literatury.

Prohlašuji, že v souladu s § 47b zákona č. 111/1998 Sb. v platném znění souhlasím se zveřejněním své disertační práce, a to v úpravě vzniklé vypuštěním vyznačených částí archivovaných Přírodovědeckou fakultou elektronickou cestou ve veřejně přístupné části databáze STAG provozované Jihočeskou univerzitou v Českých Budějovicích na jejích internetových stránkách, a to se zachováním mého autorského práva k odevzdanému textu této kvalifikační práce. Souhlasím dále s tím, aby toutéž elektronickou cestou byly v souladu s uvedeným ustanovením zákona č. 111/1998 Sb. zveřejněny posudky školitele a oponentů práce i záznam o průběhu a výsledku obhajoby kvalifikační práce. Rovněž souhlasím s porovnáním textu mé kvalifikační práce s databází kvalifikačních prací Theses.cz provozovanou Národním registrem vysokoškolských kvalifikačních prací a systémem na odhalování plagiátů.

České Budějovice, 09.09.2014 .....

Oksana Degtjarik

This thesis originated from the Faculty of Science, University of South Bohemia, supporting doctoral studies in the Biophysics study programme.

Financial support

This research was supported by the Czech Science Foundation grant P207/12/0775, Grant of the Ministry of Education of Czech Republic LO1214, Central European Institute of Technology CZ.1.05/1.1.00/02.0068.

List of publications and author's contribution

The thesis is based on the following publications (listed chronologically):

1. **O. Degtjarik***, R. Dopitova*, D. Reha, S. Puehringer, O. Otrusinova, M. Kuty, M. S. Weiss, L. Janda, L. Zidek, I. Kuta-Smatanova and J. Hejatko. Structure of Phoshotransmitter AHP2 and its interaction with the receiver domain of sensor histidine kinase CKI1 – towards specificity in the multistep phosphorelay signaling in plants. *Manuscript.* * - equal contribution

   OD performed the crystallization experiments, the data collection and processing, structure solution, the data analysis, wrote and revised the manuscript (jointly with RD and LZ).

2. K. Tratsiak, **O. Degtjarik**, I. Drienovska, L. Chrast, P. Rezacova, M. Kuty, R. Chaloupkova, J. Damborsky and I. Kuta Smatanova. Crystallographic analysis of new psychrophilic haloalkane dehalogenases: DpcA from *Psychrobacter cryohalolentis* K5 and DmxA from *Marinobacter sp*. ELB17. *Acta Cryst.* (2013). F69, 683-688. (IF = 0.6)

   OD collected and processed a part of the data, participated in writing of the manuscript.

3. **O. Degtjarik**, R. Chaloupkova, P. Rezacova, M. Kuty, J. Damborsky and I. Kuta Smatanova. Differences in crystallization of two LinB variants from *Sphingobium japonicum* UT26. *Acta Cryst*. (2013). F69, 284-287. (IF = 0.6)

   OD performed the crystallization experiments, the data collection and processing, wrote the manuscript.

4. **O. Degtjarik***, R. Dopitova*, S. Puehringer, E. Nejedla, M. Kuty, M. S. Weiss, J. Hejatko, L. Janda and I. Kuta Smatanova. Cloning, expression, purification, crystallization and preliminary X-ray diffraction analysis of AHP2, a signal transmitter protein from *Arabidopsis thaliana*. *Acta Cryst*. (2013). F69, 158-161, * - equal contribution. (IF = 0.6)

   OD performed the crystallization experiments, thermal shift assay, the data collection and processing, wrote the manuscript.

5. T. Prudnikova, R. Chaloupkova, Y. Sato, Y. Nagata, **O. Degtjarik**, M. Kuty, P. Rezacova, J. Damborsky, and I. Kuta Smatanova. Development of crystallization protocol for the DbeA1 variant of novel haloalkane dehalogenase from *Bradyrhizobium elkanii* USDA94. *Crystal Growth & Design* (2011). 11, 516-519. (IF = 4.7)
   OD participated in part of the experimental work.

Publication not included in the thesis:

1. V. Kral , Z. Antosova M. Hladikova, **O. Degtjarik**, M. Mackova, D. Stys, J. Sotola, J. Ludwig. Recombinant production of teriparatide in *Escherichia coli* bacteria, which is a biologically active fragment of human parathyroid hormone (parathormone) consisting of specified N-terminal amino acids, useful as fusion protein. (2011) Patent Numbers: CZ201000374-A3; CZ302526-B6. Accession Number: 2011-H78320 [02]

Dedicated to my family

ACKNOWLEDGEMENTS

I express my gratitude to all those people who made my dissertation possible.

Primarily, I would like to address a deep thank to my supervisor Ivana Kuta Smatanova who supported and encouraged me during all my study. I am very grateful for your patience, enthusiasm and a great atmosphere for doing research.

Many thanks I would like to address to my colleagues and collaborators: Radka Dopitova for sharing with me your deep knowledge in protein production, for your friendship and continuous support; Honza Hejatko for productive scientific discussions; Pavlina Rezacova for introducing me to the field of protein crystallography and for valuable advices; Radka Chaloupkova and Jiri Damborsky for providing the samples of haloalkane dehalogenases and for the excellent cooperation; Jost Ludwig for all molecular biology tips and tricks I have learnt from you. I express my gratitude to Manfred S. Weiss and Sandra Puehringer for helping me with the data collection and determination of AHP2 structure, for your time and support during my stay at BESSY. I thank to David Reha and Michal Kuty for showing me the world of computational biology.

I am also thankful to technical and administrative stuff of the Castle for providing me all necessary facilities to make my stay easy and comfortable.

My deep thanks belong to my friends from Nove Hrady and Ceske Budejovice: Tanya Prudnikova, Alexey Bondar, Olga Shmidt, Julia Ermak, Anna Hurina, Katya Sviridova. Thank you for listening, support, for our debates and for all the great times we shared. I am grateful to Vladik for his sincere smile that always cheers me up. I would like to thank Radka Sermina for many wonderful lunches and non-scientific discussions.

My special thanks belong to my Czech friends Katka and Honza Knezinkovi, Milan Kozeluh, Honza Kozeluh and Jonasek for your support and for the memorable moments we shared together.

Finally, I am very grateful to my parents for their constant support and sacrifices, to my brother Sergey for his equanimity, and to my nephew Timoshka for always making me laugh.

In addition, I would like to thank all the people whose names I did not mention here, but who shared with me this life-changing journey called PhD study.

CONTENTS

LIST OF ABBREVIATIONS

3D – tree-dimentional
ADP - Adenosine diphosphate
Ala, A – Alanine
Arg, R – Arginine
Asn, N – Asparagine
Asp, D – Aspartic acid
ATP - Adenosine triphosphate
cGMP - Cyclic guanosine monophosphate
Cys, C – Cysteine
Gln, Q – Glutamine
Glu, E – Glutamic acid
Gly, G – Glycine
His, H – Histidine
Ile, I – Isoleucine
Leu, L – Leucine
Lys, K– Lysine
Met, M – Methionine
NMR - Nuclear magnetic resonance
Pdb – Protein data bank
Phe, F – Phenylalanine
Pro, P – Proline
Ser, S – Serine
Thr, T – Threonine
Trp, W – Tryptophan
Tyr, Y – Tyrosine
Val, V – Valine

1. Prologue and aims of thesis

X-ray crystallography is the most powerful experimental technique for studying three-dimensional (3D) structure of proteins. This method provides the information about the location of every atom in a protein molecule based on the diffraction of X-rays by electrons of many identical molecules packed in a well-ordered crystal. Knowing the protein structure allows us to understand protein properties and function. The method of X-ray crystallography is used to determine the detailed structure of protein-ligand complexes as well as large molecular assemblies. Due to this, X-ray crystallography is widely used for clarification of enzymatic mechanisms, various protein-protein interactions and structure-guided drug design.

The first determined protein crystal structure was myoglobin in 1958 [1, 2]. Since that time atomic coordinates for over 100 000 structures of biomolecules were deposited to the Protein Data Bank (www.pdb.org). Around 90% of them are determined by X-ray crystallography, while the remaining 10% of structures are determined by NMR spectroscopy and electron microscopy.

In order to obtain accurate high resolution protein structure by X-ray crystallography a well-diffracting 3D protein crystal is required. Crystallization is the most critical step on the way of X-ray protein structure determination. To date, it is not possible to predict the exact conditions enabling formation of single crystals of a specific protein. Protein molecules by their nature are large, flexible and irregularly shaped. Therefore, to get them assembled into a regular periodic crystal lattice is not a trivial task. Despite the various methods developed during last several years, protein crystallization still remains problematic and dependent on empirical approaches [3].

This thesis is based on the experimental results of two projects. The first project is devoted to **crystallization and preliminary crystallographic analysis of selected haloalkane dehalogenases and their mutant variants**. The main goals of this project were to:

1. Find the optimal crystallization conditions for new constructed LinB32, LinB86, LinB70 mutant variants.
2. Determine the influence of physical and chemical parameters on the crystallization of mentioned haloalkane dehalogenases and their variants.

3. Solve the structure of selected haloalkane dehalogenase mutant variants in order to investigate the effect of mutations on the enzyme from the structural perspective.

The second project was aimed at **crystallization and structure solution of histidine phosphotranser protein 2 (AHP2) from *Arabidopsis thaliana*, and its interaction with the receiver domain of sensor histidine kinase CKI1**. The project had the objectives to:

1. Investigate of optimal crystallization conditions for obtaining good quality crystals of AHP2 protein suitable for X-ray diffraction analysis.
2. Solve the structure of AHP2 protein based on the diffraction data obtained from AHP2 crystals.
3. Analyze the AHP2 crystal structure and compare with the structures of histidine phosphotransfer proteins from higher plants.
4. Ascertain of the binding mode of AHP2 with its partner receiver domain of histidine kinase CKI1.
5. Identify the structural features determining binding specificity of AHP2 and $CKI1_{RD}$.

2. Introduction

2.1. Haloalkane dehalogenases

Haloalkane dehalogenases (HLDs) are a group of enzymes that catalyze a hydrolytic cleavage of carbon-halogen bond in various halogenated compounds. Some of the substrates for HLDs are produced naturally by marine organisms (chloromethane, iodomethane, bromomethane, 1,2-dibromoethane, bromopropane, etc.), volcanoes (chloromethane, bromomethane, iodomethane) and during biomass burning (chloromethane, bromomethane, [4]). However, the majority of haloalkanes and their derivatives belong to xenobiotic compounds, which were introduced into the environment by industrial activity [5, 6]. During the enzymatic reaction HLDs replace responsible for toxicity halogen atom of the substrate to hydrogen or a hydroxyl group [7]. Due to this property, HLDs can be potentially applied in biodegradation of various halogenated environmental pollutants, for detoxification of warfare agents, cell imaging, as biosensors for detection of halogenated compounds [8-11].

HLDs were originally discovered in soil and water bacteria (*Xanthobacter autothrophicus* GJ10, *Sphingobium japonicum* UT26, [12]), which use halogenated compounds as a single source of energy and carbon. However, recently presence of the enzymes was experimentally confirmed also in pathogen bacteria (*Mycobacterium tuberculosis* 5033/66, *Micobacterium avium* N85), plant symbionts (*Bradirizobium japonicum* USDA110, *Bradirizobium elkanii* USDA94, [13, 14]), plant parasites (*Agrobacterium tumefaciens* C58) and in eukaryotic organism *Strongylocentrotus purpuratus* where their function is still unclear [15, 16].

To date, over 200 of putative HLDs were identified by phylogenetic analysis, 17 of them were biochemically characterized and 3D structure of 10 of them was determined (Table 1.)

Table 1. List of experimentally characterized haloalkane dehalogenases.

HLD	Organism	PDB ID	Subfamily	Reference
DhlA	*Xantobacter autotrophicus* GJ10	2HAD	HLD-I	[17]
DhaA	*Rhodococcus rhodochorus NCIMB 13064*	1BN6	HLD-II	[18]
LinB	*Sphingomonas paucimobilis* UT26	1CV2	HLD-II	[19]
DmbA	*Mycobacterium tuberculosis* 5033/66	2QVB	HLD-II	[20]
DmbB	*Mycobacterium tuberculosis* 5033/66		HLD-I	[13]
DmlA	*Mesorhizobium loti* MAFF303099		HLD-II	[14]
DbjA	*Bradyrhizobium japonicum* USDA110	3A2M	HLD-II	[8]
DbeA	*Bradyrhizobium elkanii* USDA94	4K2A	HLD-II	[21]
DrbA	*Rhodopirellula baltica* SH1		HLD-III	[22]
DmbC	*Mycobacterium tuberculosis* 5033/66		HLD-III	[22]
DhmA	*Mycobacterium avium* N85		HLD-I	[23]
DppA	*Plesiocystis pacifica* SIR-1	2XT0	HLD-I	[24]
DmmA	*Moorea producta*	3U1T	HLD-II	[25]
DpcA	*Psychrobacter cryohalolentis* K5		HLD-I	[26]
DatA	*Agrobacterium tumefaciens* C58		HLD-II	[15]
DmxA	*Marinobacter sp.* ELB17		HLD-II	[26]
DspA	*Strongylocentrotus purpuratus*		HLD-II	[16]

2.1.1. Structure of haloalkane dehalogenases

Haloalkane dehalogenases structurally belong to the α/β-hydrolase fold family, together with other hydrolytic enzymes, such as lipases, peroxidases, hydrolases, esterases and proteases [27-29]. Structure of these enzymes consists of two domains: α/β hydrolase core domain and α-helical cap domain. A three-layer core domain is composed of central eight-stranded (7 parallel and 1 antiparallel) β-sheets, surrounded by two and four α-helices (Fig. 1).

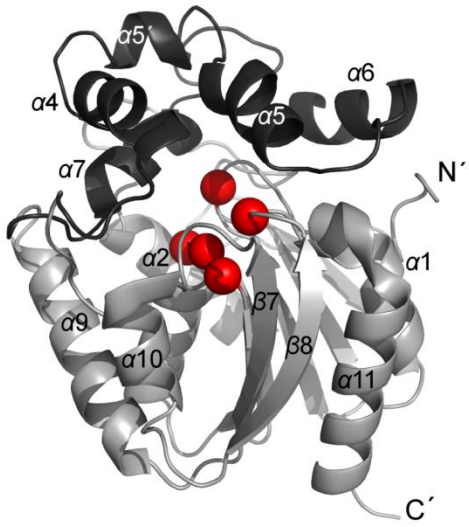

Figure 1. The overall structure of haloalkane dehalogenases exemplified by LinB enzyme. The core domain is colored by light-grey; the cap domain is colored by black. The catalytic pentad is represented by red balls.

Smaller cap domain situated between β6 and α8 covers the top of the core domain and consists of five α-helices, connected by loops [30]. Core domain serves as a framework for catalytic residues and the active site cavity [30]. Anatomy of the cap domain affects the substrate specificity of the enzymes by size and shape of the active site cavity, nature of the active site residues and physical parameters of the tunnels connecting active site cavity with protein surface [19, 30-32]. The major structural differences among all HLDs are observed in cap domain, while the structure of core domain remains conserved [33].

The interface between the core domain and the cap domain is represented mostly by hydrophobic residues, which form buried active site cavity. A catalytic pentad, responsible for the enzyme's function is situated inside the active site cavity and connected with surrounding solvent by the tunnels. The pentad consists of nucleophile (Asp), base (His), catalytic acid (Asp or Glu) and two halide-stabilizing residues (Trp and Trp or Asn, Fig.1).

Nucleophile is always located after β5 strand in very sharp turn called "nucleophile elbow" that is easily accessible for the substrate and hydrolytic water molecules. This structural feature is the most conserved within α/β-hydrolase fold [34, 35]. The position of the catalytic base His in β8-α10 loop is also conserved among all HLDs. The catalytic acid (Asp or Glu) is situated either after β6 strand or after β7 strand. The halide-binding tryptophan is situated strictly next to nucleophile. The backbone amidic group of catalytic tryptophan and amidic group from the residue located after strand β3, which is hydrogen bounded to nucleophile, form oxyanion hole. The oxyanion hole is typical structural feature for α/β-hydrolases [27, 28]. It plays an important role in stabilization of negative charge during hydrolysis [34]. The side chains of the oxyanion hole line the wall of the active site cavity. The second halide-binding residue (Trp or Asn) can be located after β3 or in α4 of the cap domain (Fig.2). The halide-binding residues are responsible for the proper orientation of the substrate in the active site [34].

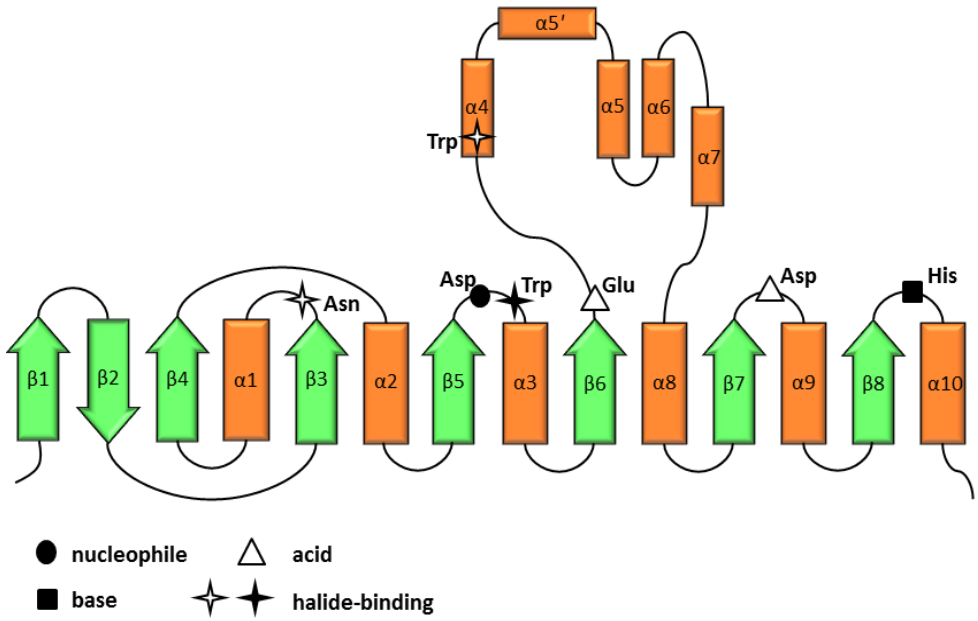

Figure 2. Topology of secondary structure elements in haloalkane dehalogenases (modified from [36]).

Based on phylogenetic analysis and composition of the catalytic pentad HLD family can be divided into three subfamilies: HLD-I (Asp-Asp-His and Trp-Trp), HLD-II (Asp-Glu-His and Asn-Trp) and HLD-III (Asp-Asp-His and Asn-Trp). The majority of biochemically and structurally characterized HLDs belong to HLD-II subfamily (Table 1).

2.1.2. Reaction mechanism of haloalkane dehalogenases

The overall reaction mechanism of HLDs was proposed from X-ray crystallography after determination of DhlA structure [37]. Various soaking experiments with the substrate under different pH values and solving of the 3D structures of the intermediates reveal a multistep reaction cycle consisting of (i) substrate binding, (ii) formation of alkyl-enzyme complex, (iii) hydrolysis of the alkyl intermediate and (iv) product release [38].

The reaction of dehalogenation is initiated after binding of the substrate to the active site. Substrate is bound by its halogen to the nitrogen atoms of two halide-stabilizing amino acid residues. The halogen-bound sp^3-hybridised

carbon atom of the substrate is faced towards nucleophilic Asp amino acid residue. One of the Asp side-chain oxygens attacks halogen-bound carbon atom resulting in formation of covalent alkyl-enzyme intermediate and halide ion, which remains associated with the side-chains of two halide-stabilizing amino acid residues. The negative charge on the second (free) carboxyl oxygen is stabilized by the oxyanion hole [32].

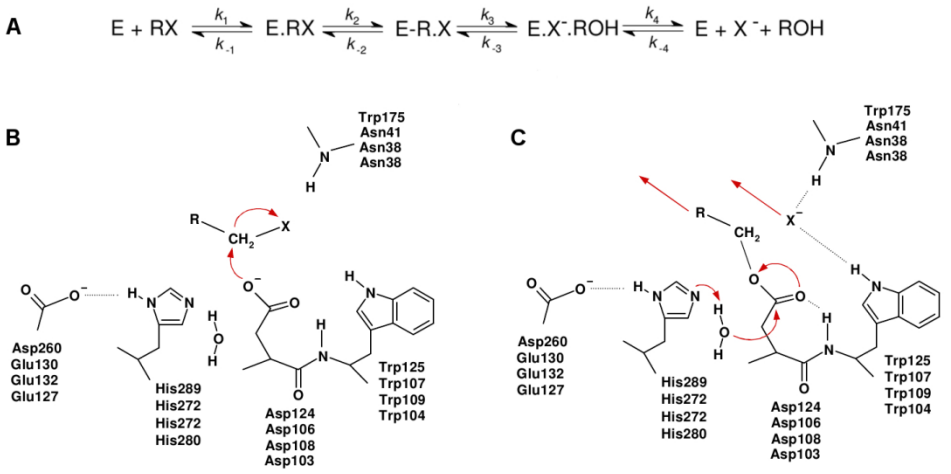

Figure 3. General catalytic mechanism of haloalkne dehalogenases. **(A)** Schematic representation of HLDs kinetic mechanism: substrate binding, formation of the alkyl-enzyme intermediate, hydrolysis of the alkyl-enzyme intermediate and release of the products from the active site. **(B)** Formation of the alkyl-enzyme intermediate. **(C)** Hydrolysis of the intermediate. Residue numbers refer to DhlA, DhaA, LinB and DbjA, respectively. X represents halogen (adapted from [36, 38]).

The next step of the reaction is the hydrolysis of covalent alkyl-enzyme intermediate by the catalytic water molecule, which is situated between nucleophilic Asp and base His. His base extracts a proton from the water molecule, thus acting as water activator. Remaining hydroxyl anion attaches to the carboxyl carbon atom of Asp nucleophile side-chain, yielding the so-called tetrahedral intermediate. Catalytic acid (Asp or Glu) plays role in stabilization of the positive charge on His by hydrogen bonding of its side-chain oxygen with His imidazole ring. The tetrahedral intermediate subsequently decomposes into alcohol and free Asp nucleophile. Hydroxyl anion provides oxygen and

proton for the alcohol product; alternatively proton can be obtained from protonated His base. The last step in the catalytic cycle is the release of all the three products: alcohol, halide ion and proton [36, 38].

The overall reaction mechanism is similar among all HLDs. The main difference is observed in the rate-limiting step of the catalytic cycle. The rate-limiting step for dehalogenation of 1,2-dichloroethane by DhlA [39] is a halide release;, for dehalogenation of 1,3-bromopropane by DhaA [38] it is a release of alcohol and hydrolysis of the alkyl-enzyme intermediate for dehalogenation of 1-chlorohexane and bromocyclohexane by LinB [35]. Rate-limiting step reflects the catalytic activity of HLDs and depends on the composition of the catalytic residues, the geometry of the active site cavity and the geometry and number of access tunnels connecting the deeply buried active site cavity with the protein surface [35, 36, 40].

2.1.3. Properties of haloalkane dehalogenases

Substrate specificity. Substrate specificity is a key characteristic of an enzyme. HLDs exhibit broad substrate specificity, converting chlorinated, brominated, iodinated alkanes, alkenes, cycloalkanes, alcohols, esters, ethers, carboxylic acids, epoxides, amides and nitriles [41, 42]. As mentioned above, substrate specificity is affected by the size, composition and architecture of the active site cavity and tunnels, connecting the active site with the surrounding solvent. Additionally, substrate specificity can be influenced by the charge distribution on the protein surface, protein solvation [43] or protein dynamics [44].

LinB, DhaA and DbjA have the largest active-site cavities of all characterized HLDs, so they are able to utilize large substrates with up to 10 carbon atoms chain length, such as monohalogenated pentanes, hexanes, heptanes, cyclopentanes and cyclohexanes [32, 42]. Small active site cavity of DhlA (112 A^3) deeply buried inside the protein cannot accommodate bulky compounds. DhlA is able to catalyze dehalogenation of only small halogenated aliphatic hydrocarbons (1,2-dichloroethane, 1,2 dibromoethane, 1-bromo-2-chloroethane, [33, 41]. Psychrophilic haloalkane dehalogenase DpcA exhibit high activity with 1-bromobutane, 1-bromohexane and 1,3-dibromopropane while no activity with chlorinated substrates, thus possessing one of the

narrowest substrate specificity profiles among all characterized dehalogenases [26].

Based on the substrate specificity profiles and relative preferences of the enzymes for thirty representative substrates the HLDs are divided into four substrate specificity groups (SSGs, [42]). SSG-I includes catalytically robust HLD, active with the most of the tested substrates (DbeA, DhaA, DhlA, LinB). SSG-II contains only DmbA enzyme, which is unique by its good activity towards not preferred substrates such as 2-iodobutane, 1-chloro-2-(2-chloroethoxy)ethane and chloro-cyclopentane. SSG-III includes DrbA, which is characterized by low or zero activity towards all of the tested compounds and high activity towards 1-chlorobutane. SSG-IV comprises of DatA, DbeA, DmbC, DpcA and DspA with preference for terminally substituted brominated and iodinated propanes and butanes [16, 26, 42].

Enantioselectivity. Haloalkane dehalogenases are capable for enantioselective conversion of racemic mixtures of different halogenated compounds (Table 2). Excellent enantioselectivity towards α-brominated esters was proven for the majority of tested dehalogenases: DhaA, DbjA, LinB [8], DatA [15], DpcA [26]. Besides, DhaA, DbjA and LinB are able to discriminate enantiomers of α-bromoamides [45]. DbjA and DatA exhibit enantioselectivity towards β-brominated haloalkanes [8, 15]. DhlA is the least enantioselective among all tested haloalkane dehalogenases, showing very weak selectivity only with 1,2 and 1,3 short chain dihaloalkanes (E = 2-4, [46]). Novel eukaryotic haloalkane dehalogenase DspA has no or very low selectivity with brominated esters, but appeares to be the most enantioselective of all biochemically characterized haloalkane dehalogenases towards 2-bromobutane and thus may be attractive for biocatalysis [16]. Enantioselectivity is usually expressed in terms of enantiomeric ratio or E value (E, the ratio of specificity constants for the preferred or non-preferred enantiomer, [47]).

2.1.4. Engineered haloalkane dehalogenases

HLDs are well characterized family of enzymes with potential application in various fields, e.g. bioremediation and biosensing of toxic environmental pollutants, detoxification of chemical warfare agents, and preparation of optically pure organic halogenated compounds, cell imaging or protein analysis

[42]. Protein engineering is a powerful tool for enhancing the desired properties, quite often limited in natural enzymes. Robustness, simple catalytic mechanism that does not require a co-factor, broad substrate specificity and enantioselectivity make HLDs an attractive target for protein engineering.

HLDs with modified activity. 1,2,3-Trichloropropane (TCP) is toxic synthetic compound of anthropogenic origin, which demonstrate strong resistance to biological and chemical degradation. It was shown that haloalkane dehalogenase DhaA can utilize TCP under laboratory conditions with very slow rate [48]. Random mutagenesis technics were applied to create a DhaA mutant (C176Y+Y273F) with 3.5-fold increased activity towards TCP than the wild type [38, 40] used rational protein design and directed evolution to create variants of DhaA with narrowed tunnels, connecting buried active site cavity with surrounding solvent. Crystal structure analysis of the mutant confirmed that narrowing of the access tunnels limits the accessibility of the active site for water molecules, which in the wild type competes with TCP for interaction with the nucleophile [49]. This strategy resulted in the mutant (I135C+C176Y+V245Y+Y273F) with 32-fold improved activity towards TCP compared to the wild type [40].

HLDs with modified substrate specificity. DhlA enzyme has small active site cavity, therefore shows high activity with di-clorinated short chain haloalkanes, but very low or no activity with >3 carbon atoms in the substrate. Four mutants were constructed using site-directed mutagenesis with a goal to enlarge active site cavity of DhlA by replacing bulky amino acids with alanine. As a result, three of four mutants (F164A, D170A, F172A) showed increased catalytic activity against substrates with longer chain length compared with the wild type [50].

Another example of engineered substrate specificity is haloalkane dehalogenase LinB isolated from *Sphingobium japonicum* UT26. Replacing of L177 lying at the tunnel opening by bulky tryptophan leads to dramatic decrease of the catalytic activity towards the best substrate 1,2-dibromoethane up to 7% of the wild type value [51].

HLDs with modified enantioselectivity. Previous studies, conducted on the cognate to HLDs Lipase A from *Bacillus subtilis,* have shown the influence of loops on enantioselectivity of the enzyme [52]. The detailed analysis of

DbjA – the most enantioselective HLD enzyme towards haloalkanes – which included protein crystallography, kinetic measurements, mutagenesis and molecular modelling, revealed that the high enantioselectivity of the enzyme is associated with the surface loop lying between the core and cap domains [8]. Deletion of this loop resulted in inclined conformation of His139, what reduces the volume of the active site cavity. These changes cause decreasing of the enantioselectivity with 2-bromopentane and increasing with methyl 2-bromobutyrate. Substitution of bulky His by small Ala restores the enantioselectivity for both substrates, demonstrating the new possibilities for the modulation of enentioselectivity in HLDs by protein engineering [8].

2.1.5. Haloalkane dehalogenase LinB

Haloalkane dehalogenase LinB is the enzyme isolated from *Sphingobium japonicum* UT26, which grows on ɣ-hexachlorocyclohexane as the sole carbon and energy source [53-55]. LinB is able to convert cyclic dienes, broad range of halogenated alkanes and alkenes to their corresponding alcohols and halide ions [55], which comprise a large group of environmental pollutants. Due its broad substrate specificity, LinB can be potentially applied for bioremediation of xenobiotic compounds.

The catalytic cycle of LinB is similar to all HLDs and was described earlier [35]. The cleavage of the carbon-halogen bond is the fastest step in catalytic cycle, while the hydrolysis of the alkyl-enzyme intermediate is rate-limiting step in the kinetic mechanism [35].

Structure of LinB is typical for α/β-hydrolase proteins. It consists of conserved α/β core domain and upper α-helical cap domain, which is sequentially and structurally varied among dehalogenases (LinB pdb id 1CV2, [19]. The core domain (residues 3-132, 214-296) consists of a central twisted eight-stranded β-pleated sheet, flanked by two on one side and four on the other side α-helices. The cap domain (residues 133-213) is formed by five α-helices (Figure 1, [19]).

LinB belongs to HLD-II subfamily [33]. The catalytic nucleophile Asp108 is situated at the "nucleophile elbow" between β5 strand and α3 helix, base His272 is located in β8-α11 loop and catalytic acid lies after strand β6. Halide stabilizing residues Asn38 and Trp109 ale located on the loops between

β3-α1 and β5-α3, respectively [19, 34]. The active site cavity of the enzyme is one of the largest among structurally characterized dehalogenases (276 A^3). Due to the large active site cavity LinB prefers to utilize long-chain and bulky substrates [53]. The deeply buried cavity of the enzyme is connected with surrounding solvent by tunnels identified by Caver program (Fig. 4; [33]): p1 (main tunnel) and p2 (slot, [51]). The main tunnel branches into two tunnels with one asymmetric opening: p1a or upper tunnel (residues Gln146, Asp147, Gly176 and Leu177) and p1b or lower tunnel (Gln146, Leu177, Ala247, Ala271 and His272, [51, 56]).

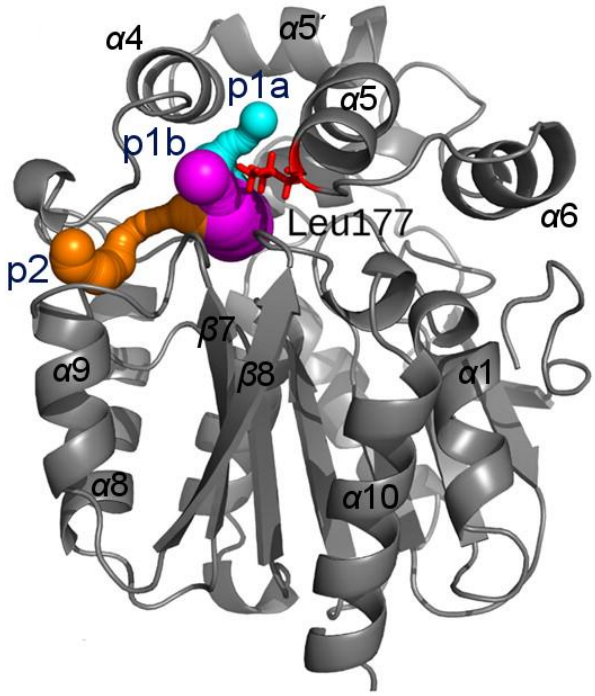

Figure 4. Crystal structure of LinB WT (PDB code 1MJ5). Tunnels are shown in sphere representation as follows: p1a tunnel (cyan), p1b tunnel (magenta), and p2 tunnel (orange). (Adapted from [51])

2.1.5.1. LinB protein variants

LinB32 and LinB86 variants. It was demonstrated that catalytic activity and substrate specificity of LinB haloalkane dehalogenase can be modulated by the residues located far from the active site [57]. Leu177 is situated at the tunnel opening and can block the access to the main tunnel (Fig. 4). This

residue was selected for the site-directed mutagenesis as the most variable among all amino acids forming the active site and access tunnels based on the sequence alignment. Replacing of Leu177 with small and nonpolar amino acids generally increased the catalytic activity of the enzyme, while introduced polar and bulky residues decreased the activity [57].

In LinB32 (L177W) variant Leu177 is replaced to bulky Trp that blocks the main tunnel entrance. The mutation causes dramatic decrease in activity of the enzyme towards the best substrate 1,2-dibromoetane [51]. Moreover, the kinetic analysis shows that introduction of the Trp at the tunnel opening changes the mechanism of bromide release from one-step process in the wild type to two-step mechanism in Leu177Trp mutant [51].

In LinB86 (W140A+F143L+L177W+I211L) variant mutations lead to the blocking the tunnel entrance and open the alternative way for the ligand and products passage.

LinB70 variant. The catalytic properties of HLDs can be affected by the composition of the catalytic residues, the geometry of the active site cavity, the geometry and dynamics of the access tunnels [35, 36, 40, 51]. Novel HLD DbeA contains the second halide-binding site, which was not previously observed in the structurally characterized HLDs. The second halide-binding site is buried in the protein core in about 10 Å far from the first binding site. Recent studies have shown that the elimination of the second halide-binding site dramatically changed catalytic activity, protein stability and substrate specificity of the enzyme [21].

LinB70 (L44I+H107Q) variant has introduced the second halide-binding site from DbeA enzyme. The variant was constructed with a goal to investigate the effect of the mutation on the enzyme properties.

2.2. Multistep phosphorelay signaling

Two-component signaling system or His-Asp phosphorelay plays an essential role in sensing/response mechanisms in both prokaryotic and eukaryotic cells [58]. In its basic form it consists of membrane-bound histidine kinase (HK) and a response regulator (RR). In response of exogenous or endogenous stimuli, histidine kinase becomes activated and autophosphorylates a conserved His residue using ATP as a phosphodonor. The phosphate signal is subsequently transferred to Asp residue of the response regulator, which usually plays a role of transcription factor [58]. Two-component signaling system exists predominantly in bacteria, where it is involved in bacterial chemotaxis [59], osmosensing [60] or nitrogen assimilation [61].

In eukaryotic microorganisms and plants two-component signaling system includes additional signaling molecules or domains and, thus, called multistep signaling system or multistep phosphorelay (MSP). MSP consists of hybrid HK, which in contrast to bacterial one carries an additional receiver domain at the C-terminus, histidine-containing phosphotransfer protein (HPt) and a response regulator. A sensory hybrid histidine kinase autophosphorylates its own His residue in response to the external stimulus. After this, the phosphoryl group is transferred to the conserved Asp residue of the HK receiver domain. HPt protein perceives the signal from receiver domain of HK and delivers it to the receiver domain of the RR (Fig. 5). The expanded phosphorelay system in eukaryotes allows performing more sophisticated regulation of signaling mechanisms and affords higher flexibility in signaling strategies compared to prokaryotic organisms. In plants, MSP participates in various key processes including hormone signaling, osmosensing [62], gametogenesis, stress and cold response [63-66].

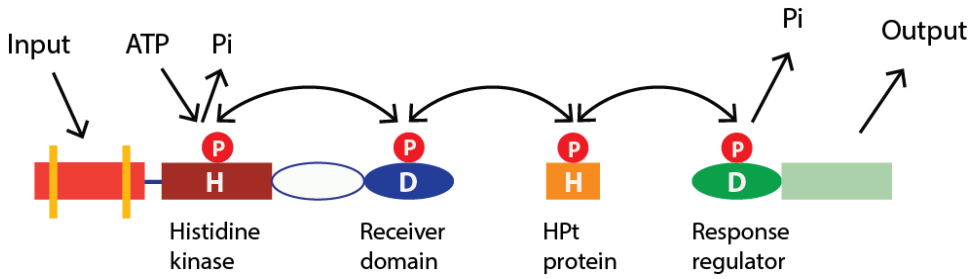

Figure 5. Schematic representation of the multistep signaling system. H – His residue, D – Asp residue, P – phosphoryl group.

Arabidopsis thaliana genome encodes 8 canonical histidine kinases (AHKs), 5 histidine-containing phosphotransmitters (AHPs), 1 pseudo-transmitter, 23 response regulators (ARRs) and 9 *pseudo*-response regulators (APRRs; [67-69]).

2.2.1. *Arabidopsis* histidine kinases

Histidine kinases in *Arabidopsis* are represented by 4 subfamilies: (i) histidine kinases (AHK2, AHK3, and AHK4), (ii) ethylene receptors (ETR1 and ERS1), (iii) cytokinin-insensitive receptors (CKI1 and CKI2 (AHK5)) and (iiii) a putative osmosensing receptor (AtHK1; [63, 68, 69]).

AHK subfamily includes tree members (AHK2, AHK3 and AHK4), which function as sensors for cytokinins [70] – plant hormones regulating cell division, growth and differentiation [71]. AHKs consist of N-terminal two or three transmembrane domains, a histidine kinase domain, a pseudo-receiver domain and a receiver domain carrying conserved Asp residue (Fig. 6; [58, 68]). Transmembrane domains are situated at the sides of conserved extracellular CHASE (**c**yclase- and **H**K-**a**ssociated **s**ensing **e**xtracellular) domain responsible for cytokinin binding [72-74]. The crystal structure of AHK4 CHASE domain in complex with cytokinin was determined by Hothorn et al. 2011 [75] (pdb id 3T4J, 3T4K, 3T4L, 3T4Q, 3T4O, 3T4S, 3T4T). Situated next to the transmembrane the kinase domain is a catalytic core of HK. It is formed by ATP/ADP-binging phosphotransfer domain and dimerization domain that contains the site of autophosphorylation. Pseudo-receiver domain is localized between histidine kinase and the receiver domain (Fig. 6). Although, structurally it is similar to the receiver domain, it cannot accept

phosphate from the conserved histidine residue. The function of the pseudo-receiver domain still remains unknown [76].

Subfamily of cytokinin-insensitive receptors includes two members CKI1 and CKI2. CKI1 does not contain CHASE domain and cannot bind cytokinins [77]. However, it is able to activate multistep phosphorelay without binding of exogenous hormones [78, 79]. In *Arabidopsis*, CKI1 is essential for gametophyte development [66, 80] and plays a role in vegetative growth [64]. However, the putative signaling molecule that interacts with CKI1 is still unknown. The crystal structure of CKI1 receiver domain ($CKI1_{RD}$) was published by Pekarova et al. (pdb id 3MMN; [81]). It is folded in central beta-sheet formed by five parallel beta-strands surrounded from the both sides by two and three alpha-helices. Aspartate residue mediating the phosphate signal is situated on the tip of β3 strand. CKI1 shows similarity with $ETR1_{RD}$ from *A. thaliana* [81].

CKI2 lacks the entire transmembrane part of the protein. CKI2 is containing only two domains – canonical histidine kinase domain and receiver domain; it is predicted to function as a cytoplasmic kinase [68, 82].

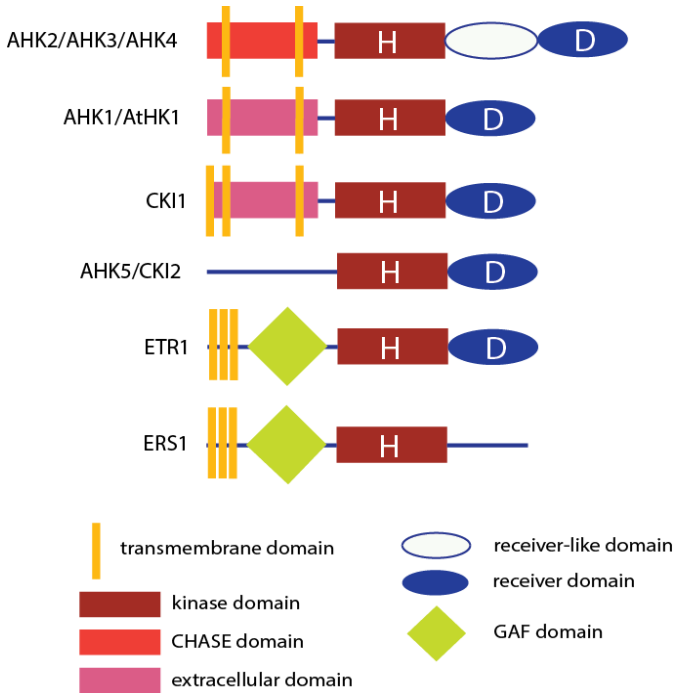

Figure 6. Domain organization of canonical histidine kinases from *A. thaliana*. H – histidine residue, D – aspartate residue (modified from [68, 69]).

Ethylene receptors family consists of two subfamilies: type-I subfamily, which includes ETR1 (ethylene resistant 1) and ERS1 (ethylene response sensor 1) and type-II subfamily, which includes ETR2, ERS2 and EIN4 (ethylene insensitive 4; [83]). Type-I subfamily of ethylene receptors contains the best studied histidine kinases in *Arabidopsis*. N-terminal of ETR1 and ERS1 is folded into 3 hydrophobic membrane-associated sensory subdomains that bind a plant hormone ethylene [84] in presence of copper as a co-factor [83]. Binding of ethylene leads to inactivation of receptor function, exhibiting negative regulation of the ethylene response pathway [85, 86]. GAF domain (named after its existence in cGMP-regulated enzymes of *Anabaena* and the bacterial transcription factor FhlA) lies between ethylene-binding domain and histidine kinase domain. GAF domains are wide-spread among different proteins and known for their ability to bind a variety of small molecules [87, 88]. Gao et al. demonstrated that GAF domain is able to mediate the interactions with other members of ethylene receptor family in *Arabidopsis* [89]. However, the exact function of GAF domain in ethylene receptors remains

unclear. C-terminal part of ETR1 and ERS1 is represented by highly conserved histidine kinase domain followed by a receiver domain with conserved phosphoaccepting Asp residue. The structure of $ETR1_{RD}$ was published in 1999, thus, representing the first crystal structure of MSP members from higher plants (pdb id 1CDF; [90]).

ERS1 lacks C-terminal receiver domain, which presents in all other members of ethylene receptor family (Fig. 6; [83]. Both ETR1 and ERS1 proteins act as homodimers, where two monomers are linked by, disulfide bridges formed between two conserved cysteins [84, 85].

As opposed, members of type-II ethylene receptors subfamily have degraded histidine kinase domain and do not exhibit histidine kinase activity [86].

AtHK1 functions as **osmosensor** in *Arabidopsis* and shows structural similarity with previously described osmosensor from yeasts SLN1 [91]. It contains three domains typical for AHKs: transmembrane domain, HK domain with conserved His residue and receiver domain with phosphoraccepting Asp residue (Fig. 6; [62]. AtHK1 responses to turgor pressure changes caused by changes of osmolarity at the surface of the cell, but the exact mechanism of AtHK1 activation is still not known [92].

2.2.2. *Arabidopsis* histidine phosphotransfer proteins

Histidine-containing phosphotransfer proteins function as signal transmitters between histidine kinase and response regulator. In the cell AHPs are localized in both cytoplasm and nucleus [93] *A. thaliana* contains six histidine phosphotransmitters (AHP1-AHP6). AHP1-AHP5 carry conserved His residue required for phosphorylation, while AHP6 is considered as pseudo-phosphotransmitter due to the lack of conserved His residue [94, 95]. AHP6 operates as inhibitor by interacting with the upstream and downstream members of phosphorelay [96]. AHP1, 2, 3 and 5 exhibit functional redundancy by acting as positive regulators of MSP signaling, whereas AHP4 in some cases plays a role of the negative regulator [95, 97]. Phylogenetically, AHP2, AHP3 and AHP5 are close to each other [95]. Also, AHP2 and AHP3 have 83% sequence identity, which is an indication of functional redundancy.

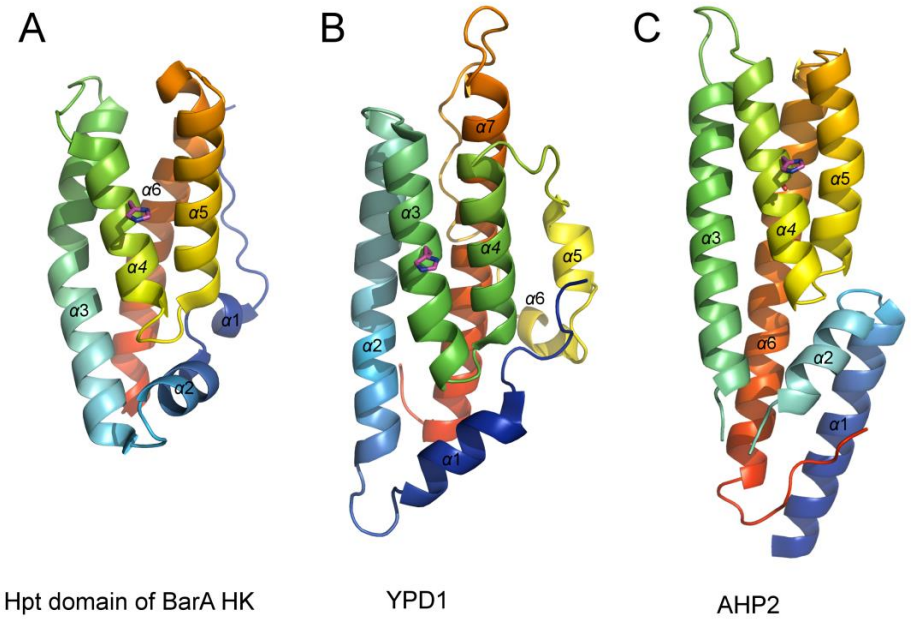

Figure 7. Cartoon representation of the tertiary structure of Hpt proteins from *E. coli* (A), *S. cerevisiae* (B) and *A. thaliana* (C). Helices are colored rainbow from N-terminus (blue) to C-terminus (red). Phosphoaccepting histidine is situated on the edge of the four-helix bundle and shown as stick.

AHPs are structurally similar to other known HPt proteins or domains from bacteria, yeasts and plants, despite quite high sequence diversity (24-55% sequence identity, Fig.7). Hpt proteins consist of about 150 amino acids and possess typical alpha-helical fold. Four helices are assembled in four-helix bundle, which contains the highly conserved XHQXKGSSXS motif with phosphosensitive His residue (Fig.7).

Structural data are available for histidine phosphotransfer proteins/domains from yeasts, bacteria, and plants (Table 3).

Table 3. List of structurally characterized histidine-containing phosphotransfer proteins.

Hpt protein/domain	Organism	PDB ID	Reference
Hpt domain of BarA HK	*Escherichia coli* CFT073	3IQT	not published
Hpt domain of ArcB HK	*Escherichia coli*	2AOB	[98]
Hpt domain of CheA HK	*Salmonella typhimurium*	1I5N	[99]
ShpA	*Caulobacter crescentus* CB15	2OOC	[100]
Ypd1	*Saccharomyces cerevisiae*	1QSP	[91]
ZmHP2	*Zea mays*	1WN0	[101]
Ak104879	*Oryza sativa*	2Q4F	[102]
MtHPt1 and MtHPt2	*Medicago truncatula*	3US6, 4G78	[103]
AHP1 in complex with AHK5	*Arabidopsis thaliana*	4EUK	[104]
AHP2	*Arabidopsis thaliana*	4PAC	[105]

2.2.3. *Arabidopsis* response regulators

ARRs (***A****rabidopsis* **r**esponse **r**egulators) are the downstream members of MSP, which catalyze the phosphate signal transfer from AHPs to its own conserved Asp residue. The phosphorylation of Asp residue results in regulation of target genes expression. First ARRs were described 16 years ago and included nine proteins (ARR1 – ARR9; [106, 107]). Nowadays ARR family includes 23 members. Based on the sequential and functional analysis all ARRs can be classified into 3 distinct groups: response regulators of type-A (ARR-A), type-B (ARR-B) and type-C (ARR-C; [108, 109]). Additional nine genes similar to those of ARRs were classified as pseudo-response regulators (APRR). APRRs do not contain conserved Asp necessary for acceptance of the phosphate signal, thus cannot function within MSP. It was shown that APRRs are involved in regulation of the circadian rhythm [110-112].

ARRs-A type counts 10 members (ARR3 – ARR9, ARR15 – ARR17). They are relatively small proteins (180 – 260 amino acids) exhibiting 50 – 93 % sequence identity in receiver domain [68, 108]. ARRs-A consist of conserved N-terminal receiver domain and a small C-terminal fragment, which function has not yet assigned [113]. Type-A ARRs can be located in cytoplasm and nucleus. The expression of *arr*-A genes is induced by cytokinins [114], indicating a possible participation of ARR-A in cytokinin signaling [68]. ARRs-A function as negative regulators of signal transduction by competing with ARRs-B for phosphoryl group mediated by AHPs [113]. Type-A response regulators are involved in pathogen [115] and temperature stress responses [116].

ARRs of type-B (ARR1, ARR2, ARR10-ARR14, ARR18-ARR21) are encoded by 11 genes. In contrast to ARRs of type-A, ARRs-B are bigger (382 – 669 amino acids) and not cytokinin inducible [117]. The response regulators of type-B contain N-terminal receiver domain with phosphorylated Asp in the center and C-terminal B-motif, comprised of DNA-binding GARP domain and glutamine-rich domain [118]. ARRs-B are located in the nucleus and function as typical transcription factors [119]. The NMR structure of ARR10 DNA-binding motif was determined fold (pdb id 1IRZ; [118]).

Later, two new members of ARR family were discovered – ARR22 and ARR24. Structurally they are similar to ARRs of type A and contain typical N-terminal receiver domain with conserved phosphor-accepting Asp residue. In contrast to ARRs of type A, ARR22 and ARR24 are not cytokinin inducible and according phylogenetic analysis they were assigned to **ARRs of type-C** group [120]. The sequences of ARR22 and ARR24 exhibit 66% of amino acid similarity, what indicates possible functional homology [121]. Several studies have shown the role of ARR-C type in cytokinin signaling pathway, but the exact function of these proteins is still not known [120, 122]. Additionally, there is one more gene that can potentially encode extra response regulator within the group (ARR23). However, according to the sequence, ARR23 has truncated phosphor-accepting receiver domain and it is still not clear whether ARR23 acts as a response regulator or not [120].

2.2.4. Interactions within *Arabidopsis* MSP pathway

Understanding the specificity of interaction between members of *Arabidopsis* MSP pathway lies in the core of studying response mechanisms in plants. AHP proteins accept the signal from the receiver domain of histidine kinase and pass it to the receiver domain of response regulator, thus AHP proteins can interact with upstream and downstream partners in MSP pathway.

By employing yeast two-hybrid system the interaction between selected AHPs (AHP1, AHP2, AHP3, AHP5) and AHKs (AHK2, AHK3 and AHK4) was detected. Furthermore, all tested AHPs interact with almost all ARRs of type A and B (Fig.8). These results indicate a high degree of functional redundancy within MSP pathway [123].

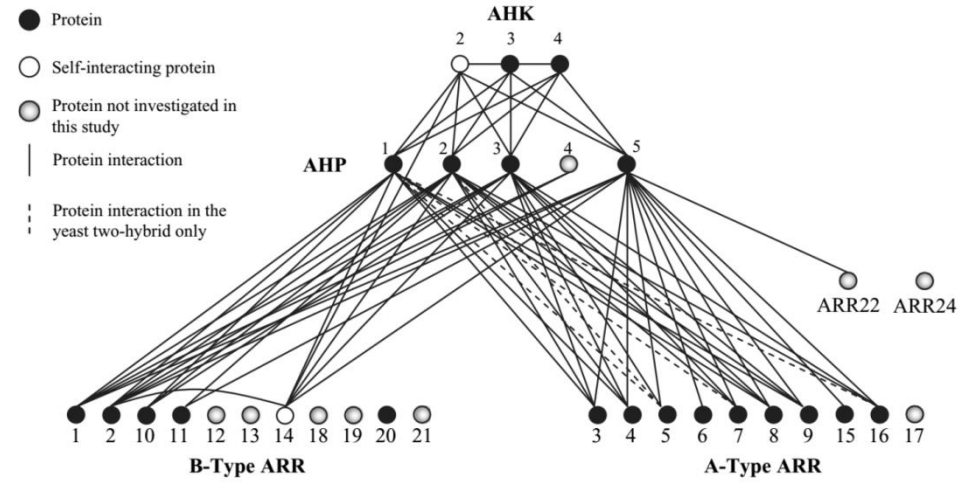

Figure 8. Protein-protein interaction network of the cytokinin signaling pathway in *Arabidopsis thaliana*. Image courtesy of Dortay et al., 2006 [123].

Interaction studies of CKI1 histidine kinase with the downstream partners were carried out using different methods. It was shown that receiver domain of CKI1 ($CKI1_{RD}$) can interact with radioactively phosphorylated AHP2 and AHP3 [124]. Furthermore, two *in vivo* methods – yeast two-hybrid system and biomolecular fluorescence complementation (BiFC) – demonstrate that CKI1 interacts with AHP2, AHP3 and AHP5 with different affinities. The strongest interaction of CKI1 was observed with AHP2 and AHP3 and weak interation with AHP5. The interaction of CKI_{RD} with AHP1, AHP4 and AHP6 was not

detected [81]. According Plasmon surface resonance studies confirmed by BiFC AHK5 can interact with AHP2, AHP3 and AHP5 with similar affinities [104]. Additionally, BiFC experiments show the interaction of AHP2 with AHP1 and AHP6, but not with AHP4 [104]. These studies point out the existence of specific preference of AHKs in choosing AHP protein as interaction partner.

AHP proteins are also able to interact with ethylene receptors. The interaction was confirmed between sensor kinase ETR1 and AHP1-3 by using yeast two-hybrid system [114]. Formation of the stable complex between ETR1 and AHP1 was confirmed by fluorescence polarization studies [125]. The interaction between ETR1 and AHP1 is modulated by the phosphorylation state of the proteins. The phosphorylation of one of the proteins causes the formation of tight ETR1-AHP1 complex. When the both proteins are either in phosphorylation or non-phosphorylation form, the interactions in the complex are much weaker [126].

3. Materials and methods

The determination of protein structure includes several stages: (i) selection of the target molecule; (ii) cloning, expression and purification; (iii) collection of diffraction data and (iv) phasing and determination of atomic coordinates (Fig. 9).

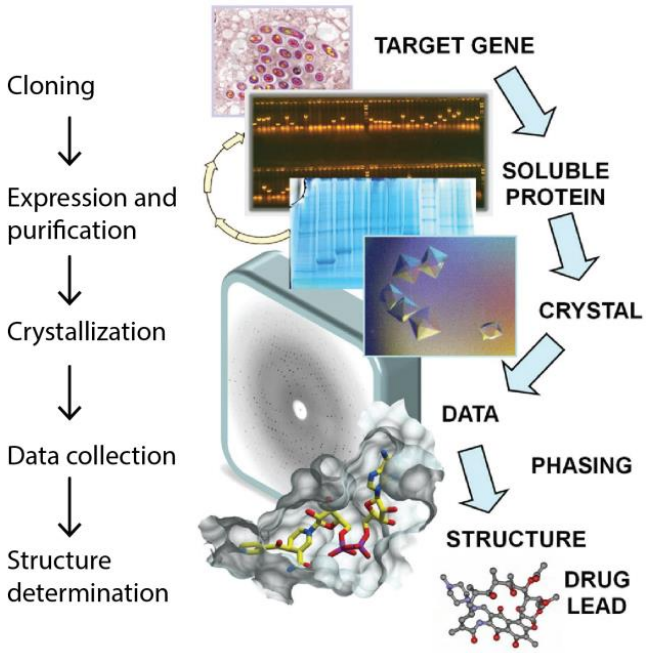

Figure 9. Overview of protein structure determination stages (modified from [127]).

First of all a highly pure, homogeneous and biologically active form of the protein should be produced. After this is fulfilled crystallization begins. Recent achievements such as automated dispensers and image captures were able to reduce time for crystallization set up and inspection of the crystallization trials from days to minutes [128]. Thousands of crystallization conditions can be tested using just few hundred nanoliters of a sample. However, crystallization is still the most critical step in protein X-ray crystallography (Fig. 10). Frequently only poor crystals observed after initial screening and the crystallization conditions need to be further optimized in order to obtain a well-diffracting crystal. Once the crystal is harvested the data

collection begins followed by solving phase problem and structure determination.

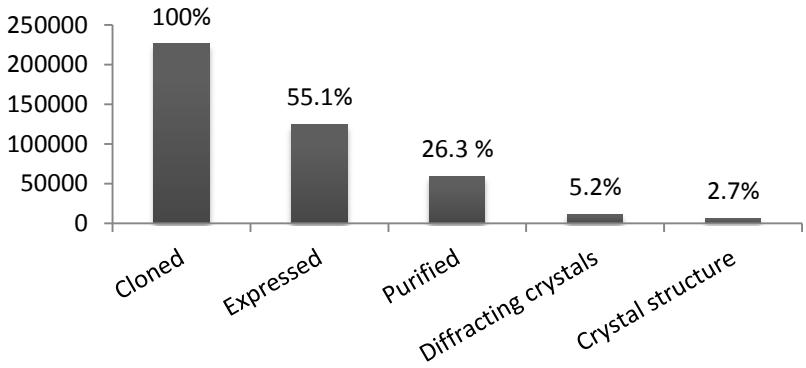

Figure 10. The statistic of the attrition at each stage of macromolecular structure determination. The graph shows the sum of the results from 17 structural genomics projects worldwide on July 2014 taken from targetdb.pdb.org.

The methods applied in this research are thoroughly described in enclosed publications. Herein, the theoretical aspects of protein crystallization and X-ray crystallography are introduced.

3.1. Protein crystallization

Having a high-quality protein crystal is necessary requirement for X-ray structure determination. The main principle of the crystallization is to induce the supersaturation in a protein solution by manipulating with physical and chemical parameters (protein concentration, pH, temperature, nature and concentration of the precipitant and others). In the supersaturated thermodynamically metastable state protein molecules can overcome an energy barrier, separate from solution and self-assemble into a periodic three-dimensional array. This is the first step of crystallization called nucleation. The second step, crystal growth starts spontaneously, after nucleus of critical size has formed [127-129].

The process of protein crystallization can be described by phase diagram (Fig. 11). The phase diagram is obtained experimentally and shows the solubility of the protein as a function of precipitant concentration in an ideal

crystallization experiment [129, 130]. The precipitant could be any chemical or physical variable that affects protein solubility. In an undersaturated region the conditions are unfavorable for nucleation or crystal growth due to very low protein and/or precipitant concentrations. The solubility curve is a border between undersaturation and supersaturation regions. It represents the dynamic equilibrium in crystallization experiment. The metastable zone supports the crystal growth, but not nucleation. In the absence of the nucleant in this zone the solution will remain clear. The next supersaturation level is nucleation zone favorable for spontaneous homogeneous nucleation. The closer system to precipitation zone – the more nuclei will appear, resulting in numerous low-quality crystals growth. When nuclei have formed, the concentration of protein in the solution will decrease leading the system to metastable zone. The process of crystal growth continues till the system will reach the dynamic equilibrium. At very high level of supersaturation protein precipitation occurs. This region is unfavorable for crystallization, because the precipitates form faster than the crystals [128, 131-133].

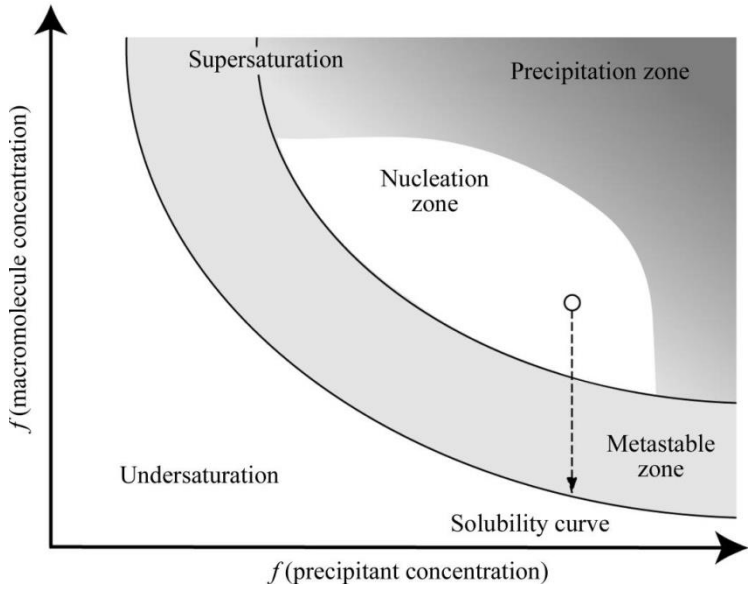

Figure 11. Simplified phase diagram for protein crystallization. The protein concentration is represented as a function of the concentration of precipitant agent. Adapted from [134].

3.1.1. Crystallization techniques

Numerous techniques have been developed for the crystallization of macromolecules: vapor diffusion (hanging-drop and sitting-drop), batch, microbatch under the oil, microdialysis, free-interface diffusion, counter-diffusion (Fig. 12).

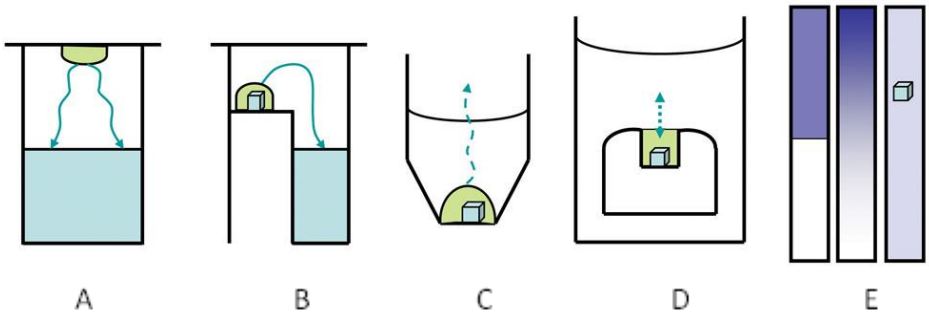

Figure 12. Schematic representation of common crystallization techniques: hanging-drop vapor diffusion (A), sitting-drop vapor diffusion (B), microbatch under oil (C), microdialysis (D), free-interface diffusion (E). Adapted from [127].

Vapor diffusion (sitting-drop, hanging-drop and sandwich drop) is the favorite technique of the most protein crystallographers. In hanging-drop method (Fig. 12A), a small droplet of the protein solution is mixed with a droplet of the precipitant solution and placed on a cover slide. The cover slide is flipped and sealed over the reservoir containing the precipitant solution (Fig. 12). In the resulting isolated system the concentration of the precipitant in the reservoir is higher. Due to the difference in the concentrations the reservoir absorbs water from the drop through the vapor and drives the solution to the supersaturation state, thus enabling crystallization. Sitting-drop method (Fig. 12B) has the same principle as hanging-drop, except that the drop is placed on concave sitting drop post and the system is isolated by a transparent sealing tape.

Both sitting-drop and hanging-drop methods are suitable for initial crystallization screening as well as for optimization of the discovered conditions. Sitting-drop vapor diffusion method was optimized for automated robotic systems, which allow minimizing the sample volume and provide high-throughput screening of crystallization conditions within several minutes [135].

Batch crystallization technique is the simplest and fastest method for protein crystallization. The principle is that the addition of the precipitant to the protein solution suddenly brings the drop to the supersaturation state. The modification of the batch technique is microbatch under oil (Fig. 12C), where the drop containing mixed protein and precipitant solutions is covered by oil [136]. The oil does not interact with common precipitants and prevents water evaporation. Mixing of water-permeable silicon oil with paraffin oil promotes evaporation of water from the drop, and thus supersaturation. Advantages of batch method include minimization of protein and precipitant volume, avoiding of condensation during temperature fluctuations and possibility of using automated systems for high-throughput crystallization screening [127].

The basis of the microdialysis technique (Fig. 12D) is that the sample is separated from a large volume of precipitant by semipermeable membrane which allows water and small molecules to pass but prevents passing of protein macromolecules. Equilibration kinetics depends on the size of membrane pores, the concentration of the precipitant inside and outside of the microdialysis cell, temperature and the geometry of the cell. The benefit of this method is that the precipitant solution can be easily exchanged. The disadvantages include tricky set up and quite big sample consumption per trial [127].

In free-interface diffusion technique (Fig. 12E), the protein and precipitant solutions contact each other in a narrow glass capillary without premixing. Over a time, two solutions diffuse to each other creating a gradient of protein/precipitant concentrations along the capillary length [137]. Similar to the free-interface diffusion is counter-diffusion technique. The example of this technique is the gel acupuncture method, where microcapillaries containing protein solution are inserted into a gel, which is covered by a layer of precipitant. The precipitant diffuses to the gel and form a gradient in microcapillary promoting crystallization along its length [138]. The diffusion time of the precipitant through the gel to the capillary can be regulated by the penetration depth of the capillary in the gel.

3.1.2. Optimization strategies

Initial screening of crystallization conditions does not always lead to getting of diffraction-quality crystals. Very often many “crystal formation” but not well-shaped crystals could be observed under stereomicroscope during the inspection of crystallization plates (Fig. 13). In order to improve crystal size and quality different optimization strategies can be applied:

1. **Fine-tuning of initial crystallization conditions.** Variation of the precipitant concentration, pH, incubation temperature, protein concentration and protein/precipitant ratio in the drop can affect crystal size and quality.

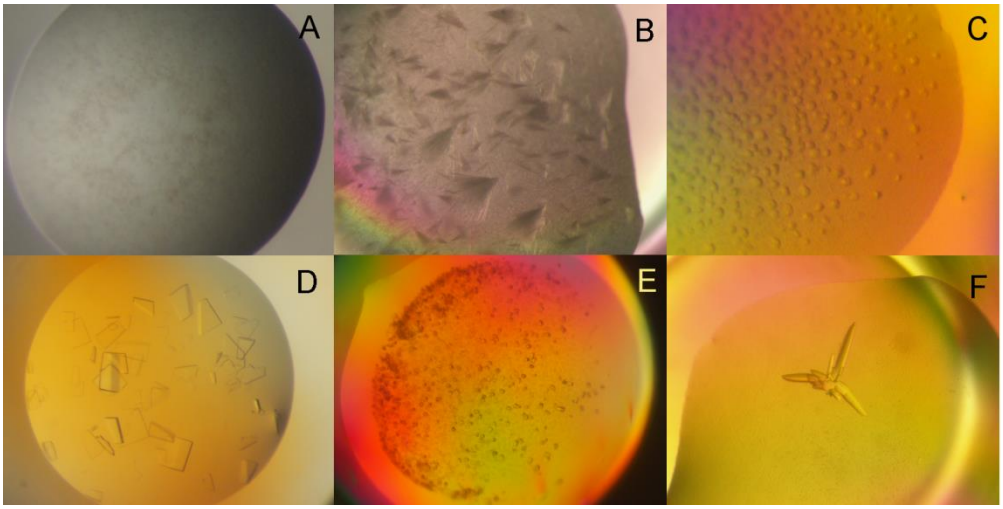

Figure 13. Outcomes of different crystallization experiments (obtained in our laboratory). A – light precipitation; B – needle clusters of LinB70; C – spherulites of LinB81; D – thin plates of the motor subunit of EcoR1241 restriction enzyme; E – microcrystals of aldehyde dehydrogenase; F – rod clusters of aldehyde dehydrogenase.

2. **Using of additives.** Additive is a chemical compound that facilitates protein crystallization. Additives may be already present in the precipitant solution or extra-added to the macromolecule solution. According to their usage, additives are classified into metal cations, small alcohols, detergents, reducing agents, etc. Addition of metal cations can improve protein crystallization by promotion of intermolecular interactions [139]. Detergents act as stabilizing agents and increase the solubility of the protein [140]. Reducing agents such as β-mercaptoethanol and dithiothreitol stabilize the protein by

preventing cysteines oxidation and these are frequently added into protein during the protein preparation [141]. Moreover, physiological ligands, cofactors, substrates and inhibitors can function as stabilizing agents and improve crystal quality compared to apo-protein.

3. **Seeding.** The main principle of the seeding technique is to introduce existing nucleus (seed) to the crystallization drop equilibrated at low level of supersaturation, which is optimal for crystal growth, but adverse for spontaneous nucleation. Seeding can be applied for initial screening as well as for increasing the size and quality of the crystals [142]. Based on the size of the seeds two main seeding methods are distinguished: macroseeding and microseeding. Microseeding implies transfer of crystal fragments crushed by vortex, seed beads, glass rods or other tools. A modification of microseeding is streak seeding, where seeds are transferred by streaking with whisker or fiber through the new drop. During macroseeding single but small crystal is washed and transferred to new crystallization drop in attempt to increase crystal size.

3.2. Crystal structure determination

3.2.1. Crystal geometry

Crystal is a three-dimensional periodic arrangement of molecules organized in a crystal lattice. The molecules are held together within a crystal by weak non-covalent interactions. Protein crystal consists of repeating building blocks called **unit cells**, which contain all the structural and symmetry information (Fig.14). Unit cell is defined by length of the cell edges (*a*, *b* and *c*) and angles between them (α, β and γ) [127].

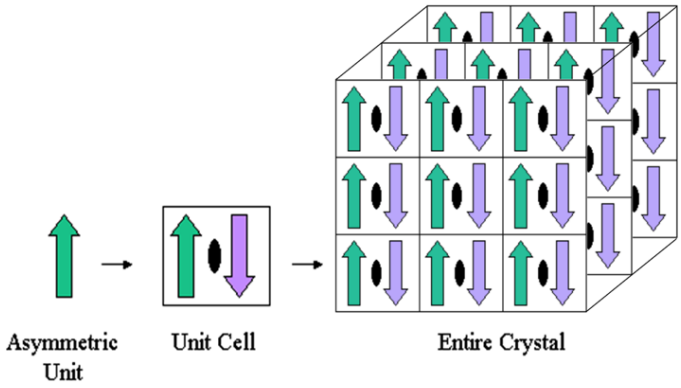

Figure 14. Relationship between asymmetric unit, unit cell and whole crystal. Asymmetric unit (green arrow) by 180° rotation around two-fold crystallographic symmetry axis (black oval) produces the second copy (violet arrow). Two arrows together comprise the unit cell. A 3D crystal is built by transitional repetitions of the unit cell in three directions. Image courtesy of *www.rcsb.org*

The smallest unit of crystal needed to reproduce the whole unit cell by applying crystallographic symmetry operations is called **asymmetric unit** (Fig.14). In protein crystallography only rotation, translation or screw axes (combination of rotation and translation) symmetry operations are allowed [143].

The internal symmetry of the unit cell and its content is described by its **space group**. Space groups belong to seven crystal systems: triclinic, monoclinic, orthorhombic, trigonal, tetragonal, hexagonal and cubic). Totally, there are 230 possible space groups. However, biological macromolecules can crystallize only in 65 of them. Knowledge of the space group and dimensions of the unit cell are essential for the interpretation of the diffraction data [143].

3.2.2. X-ray data collection

Data collection from a crystal is the last experimental step of protein structure determination process. It requires careful preparation and accuracy, because the quality of collected data determines the quality and information value of the resulting protein structure.

Data from a crystal are collected using an intense source of X-rays (laboratory with X-ray difractometer or synchrotron source). The process starts

by mounting the crystal from a crystallization drop by a cryoloop, which is secured to a pin with a magnetic base. During the mounting, crystals need to remain in the mother liquor in order to prevent desiccation and further disintegration of crystal. Data collection usually takes place under cryogenic temperatures. For this, after the mounting, the cryoloop with the crystal is flash-cooled in liquid nitrogen or directly attached to a goniometer head supplied with cryostream. The method requires pre-soaking of crystals in cryoprotectant solution to avoid the formation of crystalline ice, which destroys quality of the diffraction. The cooling of crystals under liquid nitrogen temperature minimizes X-ray radiation damage and prolongs the crystal lifetime.

For the data collection a cryoloop with the crystal is attached to a goniometer head, which allows orienting the crystal in an X-ray beam. Goniometer head is situated in the path of the X-ray beam between the radiation source and the detector. X-rays produced by the radiation source are directed on the crystal and subsequently scattered by the electrons of every atom in the crystal in many directions. Scattered X-rays interfere with each other when in phase to produce the diffraction pattern of regularly arranged spots (reflections) on the detector (Fig. 15). The measured intensities of the spots contain the information about the arrangement of molecules within a protein crystal in atomic detail [143].

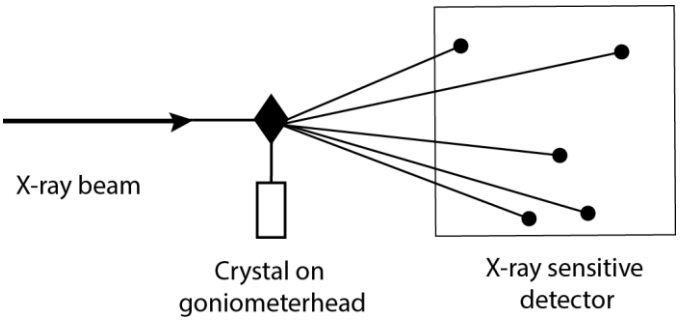

Figure 15. Schematic representation of X-ray diffraction experiment.

To obtain complete data it is necessary to obtain as many reflections as possible. This can be achieved by the rotation of the crystal around single axis with small increments (0.1-1°) while exposed to X-rays. The result of the data

collection is a set of diffraction images with recorded intensities for each single reflection and the position of reflections.

3.2.3. Protein structure solution and phase problem

The reflections obtained after the data collection can be characterized by a structure factor. **Structure factor (F_{hkl})** is a complex number that represents the total scattering from all atoms of the unit cell and includes structure factor amplitude ($|F_{hkl}|$) and a relative phase angle (Φ_{hkl}) between the diffracted waves.

The main objective of the X-ray crystallography is to calculate an **electron density map** (distribution of electrons in space), which allows to obtain the coordinates of atoms in the protein molecule. The relationship between the structure factor and electron-density map can be mathematically expressed through **Fourier transformation**, where the structure factors containing information about amplitudes and phases are used as Fourier coefficients to generate the electron density map of the protein [143]:

$$\rho(xyz) = \frac{1}{V} \sum_{hkl}^{+\infty} |F(hkl)| \cdot e^{-2\pi i[hx+ky+lz-\phi(hkl)]}$$

Amplitudes — Phases?

Symbol ρ represents the density of electrons per unit volume at any point (x, y, z), V - is the volume of the unit cell, hkl – are reflection indices. The structure factor amplitudes $|F_{hkl}|$ can be calculated as the square roots of the measured intensities (I_{hkl}). But no information about phases (Φ_{hkl}) can be obtained experimentally. This is the main problem of X-ray crystallography called the **phase problem** [143].

There are several methods to solve the phase problem and determine the structure of a protein: molecular replacement, isomorphous replacement, anomalous dispersion, isomorphous replacement with anomalous scattering, radiation damage-induced phasing. They are discussed below in brief.

1. **Molecular replacement (MR).** This is the most rapid and frequently used method for solving protein structure. The phases are obtained from the known structure of a protein, which is homologous to the unknown protein and

has similar fold and sequence. The main challenge of MR is the correct transfer of the known molecule to the unit cell of the unknown molecule. It can be achieved by two steps: rotation and translation. During the rotation the spatial orientation of the known and unknown molecules with respect to each other is determined. In the step of translation the movement required to superimpose one molecule onto the other keeping the orientation found during the rotation step is calculated [144].

2. **Isomorphous replacement (IR).** To determine the protein structure by IR method it is necessary to obtain diffraction data not only from the native protein crystal, but also from the crystal of single (SIR) or multiple (MIR) heavy atom derivatives. Incorporation of heavy atoms into the protein crystal can be achieved by crystal soaking or co-crystallization with the heavy atoms. The native and derivative crystals should have the same dimensions of the unit cells, thus they should be isomorphous. In this method the differences in the structure factor amplitudes between native (FP) and derivative (FPH) protein crystals are used to identify the positions of the heavy atoms (FP-FPH). The resulting heavy atom structure (FH) can be used as a reference structure for phase determination. Phase determination with SIR leading to two possible solutions (phase ambiguity), while using of MIR unambiguous phase determination can be achieved [145].

3. **Single and multiple anomalous dispersion (SAD and MAD).** Application of this method requires presence of strong anomalously scattering atoms, which can be incorporated into the protein (e. g. seleno-methionine derivative or metal-containing proteins) or soaked into a crystal (heavy atoms, halogens, lanthanides, ets.). Anomalous scattering properties of elements occur at specific wavelengths, which are close to the absorption edge of the element. In case of a MAD experiment up to four data sets are collected at several wavelengths around the absorption edge of the element, where the anomalous scattering factors of the element significantly different from each other. In the SAD method just one dataset is collected at the wavelength corresponding to the absorption peak of the element. The phases are derived using the differences in structure factor amplitudes arising from anomalous scattering. These differences are generally smaller than in case of IR, thus require accurate measurement of intensities during the data collection [146, 147].

4. **Single and multiple isomorphous replacement with anomalous scattering (SIRAS and MIRAS).** SIRAS and MIRAS are combination of IR and anomalous dispersion. Using of anomalous scattering can break the phase ambiguity in the SIR experiment.

5. **Radiation damage-induced phasing (RIP).** This phasing method is based on the specific effects of X-ray- or UV-induced radiation damage to protein crystals. In this experiment two datasets are collected from a single crystal with the so-called burn dose, where the crystal is exposed to high doses of X-rays or UV, in between. Radiation damage can cause significant differences in intensities between two datasets. These differences can be used for determination of phases by a SIR-type method. RIP method works well for proteins, which contain disulfide bridges [148, 149].

Protein structure determination is followed by the structure **refinement**. Refinement is represented by iterative cycles of map calculation and model building in attempts to improve the agreement between the model and observed data. The final well refined structure is then deposited in the form of atomic coordinates list to the Protein Data Bank (www.pdb.org) usually together with the final structure factors to make it available for larger community of scientists.

4. Results and discussion

4.1. PART I.

4.1.1. Differences in crystallization of two LinB variants from *Sphingobium japonicum* UT26

This chapter is based on paper:

O. Degtjarik, R. Chaloupkova, P. Rezacova, M. Kuty, J. Damborsky and I. Kuta Smatanova. Differences in crystallization of two LinB variants from *Sphingobium japonicum* UT26. *Acta Cryst*. (2013). F69, 158-161.

ABSTRACT

Haloalkane dehalogenases are microbial enzymes that convert a broad range of halogenated aliphatic compounds to their corresponding alcohols by the hydrolytic mechanism. These enzymes play an important role in biodegradation of various environmental pollutants. Haloalkane dehalogenase LinB isolated from a soil bacterium Sphingobium japonicum UT26 has a relatively broad substrate specifity and can be potentially used in bioremediation, decontamination of warfare agents and biosensing of environmental pollutants. Herein presented LinB variants, LinB32 and LinB70, were constructed with a goal to study the effect of mutations on enzyme functionality. In the case of LinB32 (L117W), the introduced mutation leads to blocking of the main tunnel, connecting the deeply buried active-site with surrounding solvent. The other variant, LinB70 (L44I + H107Q) has introduced the second halide-binding site in the position analogous to related haloalkane dehalogenase DbeA from Bradyrhizobium elkanii USDA94. Both LinB variants were successfully crystallized and full data sets were collected for native enzymes as well as their complexes with the substrates 1,2-dibromoethane (LinB32) and 1-bromobutane (LinB70) to the resolutions ranging from 1.6 Å to 2.8 Å. The two mutants crystallize differently from each other, which suggest that the mutations although deep inside the molecule, still have effects on the protein crystallizability.

4.1.2. Structural analysis of LinB32 and LinB86 haloalkane dehalogenase mutants

Unpublished results

4.1.3. Crystallographic analysis of new psychrophilic haloalkane dehalogenases: DpcA from *Psychrobacter cryohalolentis* K5 and DmxA from *Marinobacter sp.* ELB17.

This chapter is based on paper:

K. Tratsiak, **O. Degtjarik**, I. Drienovska, L. Chrast, P. Rezacova, M. Kuty, R. Chaloupkova, J. Damborsky and I. Kuta Smatanova. Crystallographic analysis of new psychrophilic haloalkane dehalogenases: DpcA from Psychrobacter cryohalolentis K5 and DmxA from Marinobacter sp. ELB17. Acta Cryst. (2013). F69, 683-688.

ABSTRACT

Haloalkane dehalogenases are hydrolytic enzymes with a broad range of potential practical applications such as biodegradation, biosensing, biocatalysis and cellular imaging. Two newly isolated psychrophilic haloalkane dehalogenases exhibiting interesting catalytic properties, DpcA from *Psychrobacter cryohalolentis* K5 and DmxA from *Marinobacter sp.* ELB17, were purified and used for crystallization experiments. After the optimization of crystallization conditions, crystals of diffraction quality were obtained. Diffraction data sets were collected for native enzymes and complexes with selected ligands such as 1-bromohexane and 1,2-dichloroethane to the resolution ranging from 1.05 Å to 2.49 Å.

4.1.4. Development of crystallization protocol for the DbeA1 variant of novel haloalkane dehalogenase from *Bradyrhizobium elkani* USDA94

This chapter is based on paper:

T. Prudnikova, R. Chaloupkova, Y. Sato, Y. Nagata, **O. Degtjarik**, M. Kuty, P. Rezacova, J. Damborsky, and I. Kuta Smatanova. Development of crystallization protocol for the DbeA1 variant of novel haloalkane dehalogenase from *Bradyrhizobium elkani* USDA94. *Crystal Growth & Design* (2011). 11, 516-519.

ABSTRACT

The DbeA1 variant of a novel haloalkane dehalogenase DbeA (EC 3.8.1.5) from *Bradyrhizobium elkani* USDA94 was constructed to study the structure-function relationships between DbjA and DbeA enzymes. A DbeA1 variant carries a unique fragment of nine amino acids transplanted from the sequentially closely related enzyme DbjA from *Bradyrhizobium japonicum* USDA110 to DbeA. Here we report development of the crystallization protocol for DbeA1 and soaking experiments with the ligands 1-fluoropentane and 1,3-dichloropropane.

4.2. PART II.

4.2.1. Cloning, expression, purification, crystallization and preliminary X-ray diffraction analysis of AHP2, a signal transmitter protein from *Arabidopsis thaliana*.

This chapter is based on paper:

O. Degtjarik*, R. Dopitova*, S. Puehringer, E. Nejedla, M. Kuty, M. S. Weiss, J. Hejatko, L. Janda and I. Kuta Smatanova. Cloning, expression, purification, crystallization and preliminary X-ray diffraction analysis of AHP2, a signal transmitter protein from *Arabidopsis thaliana*. Acta Cryst. (2013). F69, 158-161, * - equal contribution.

ABSTRACT

Histidine-containing phosphotransfer proteins (HPts) from *Arabidopsis* thaliana (AHP1-5) act as intermediates between sensor histidine kinases (HK) and response regulators (RR) in a signalling system called multistep phosphorelay (MSP). AHP proteins mediate and potentially integrate various MSP-based signaling pathways (e.g. cytokinin or osmosensing). However, structural information about AHP proteins and its importance in the MSP signaling is still missing. To get deeper insight into the structural basis of the AHP-mediated signal transduction, we set out to determine the three-dimensional structure of AHP2 protein. The AHP2 coding sequence was cloned into pRSET B expression vector enabling production of AHP2 fused to an N-terminal His tag. AHP2 was expressed in soluble form in BL21(DE3) pLysS E.coli strain and then purified into the homogeneity using metal chelate affinity chromatography and anion exchange chromatography under reducing conditions. Successful crystallization in a buffer, which was optimized for thermal stability yielded crystals diffracting to 2.5 Å resolution.

4.2.2. Structure of phoshotransmitter AHP2 and its interaction with the receiver domain of sensor histidine kinase CKI1 – towards specificity in the multistep phosphorelay signaling in plants.

This chapter is based on paper:

O. Degtjarik*, R. Dopitova*, D. Reha, S. Puehringer, O. Otrusinova, M. Kuty, M. S. Weiss, L. Janda, L. Zidek, I. Kuta-Smatanova and J. Hejatko. Structure of Phoshotransmitter AHP2 and its interaction with the receiver domain of sensor histidine kinase CKI1 – towards specificity in the multistep phosphorelay signaling in plants. *Manuscript.* * - equal contribution

ABSTRACT

In *Arabidopsis*, histidine phosphotransfer proteins (HPts) play a role of signal transmitters between diverse senor histidine kinases and response regulators within multistep phosphorelay (MSP) pathway. Previously reported ability of HPts to interact with the receiver domains of sensor histidine kinases with different affinities indicates on the certain specificity of the interaction between two partners. In order to explore the determinants of the interaction specificity between AHP2 and the receiver domain of histidine kinase CKI1 ($CKI1_{RD}$) at molecular level, we determined the three-dimensional structure of AHP2 by experimental phasing at 2.53 Å resolution. Molecular dynamic simulations for 100 ns were applied to identify the key residues responsible for the AHP2-$CKI1_{RD}$ interaction. The AHP2-$CKI1_{RD}$ interaction was confirmed by NMR measurements and resulting chemical shifts partially overlap with the model. AHP2-$CKI1_{RD}$ model reveal strong protein-protein complex; the comparison of the model with recently published crystal structure of AHP1-

$AHK5_{RD}$ suggests significant differences in binding interface between both complexes, mostly in the amino acid residues mediating hydrophilic interactions. Due to the fact that the vast majority of interacting residues in AHP1 and AHP2 are represented by highly conserved residues, small structural differences of both AHPs and AHK_{RD}s seem to be sufficient for determination of specific molecular recognition as could be seen by our bioinformatical and structural comparisons.

4. Conclusions

5. References

1. Kendrew, J.C., et al., *A three-dimensional model of the myoglobin molecule obtained by x-ray analysis.* Nature, 1958. **181**(4610): p. 662-6.
2. Dickerson, R., J.C. Kendrew, and B.E. Strandberg, *Crystal Structure of Myoglobin - Phase Determination to a Resolution of 2a by Method of Isomorphous Replacement.* Acta Crystallographica, 1961. **14**(11): p. 1188-&.
3. McPherson, A., *A comparison of salts for the crystallization of macromolecules.* Protein Science, 2001. **10**(2): p. 418-422.
4. Gribble, G.W., *The diversity of naturally produced organohalogens.* Chemosphere, 2003. **52**(2): p. 289-297.
5. Nagata, Y., et al., *Purification and characterization of a haloalkane dehalogenase of a new substrate class from a gamma-hexachlorocyclohexane-degrading bacterium, Sphingomonas paucimobilis UT26.* Applied and Environmental Microbiology, 1997. **63**(9): p. 3707-3710.
6. Copley, S.D., *Microbial dehalogenases: enzymes recruited to convert xenobiotic substrates.* Current Opinion in Chemical Biology, 1998. **2**(5): p. 613-617.
7. Janssen, D.B., F. Pries, and J.R. Vanderploeg, *Genetics and Biochemistry of Dehalogenating Enzymes.* Annual Review of Microbiology, 1994. **48**: p. 163-191.
8. Prokop, Z., et al., *Enantioselectivity of haloalkane dehalogenases and its modulation by surface loop engineering.* Angew Chem Int Ed Engl, 2010. **49**(35): p. 6111-5.
9. Furukawa, K., *Oxygenases and dehalogenases: Molecular approaches to efficient degradation of chlorinated environmental pollutants.* Bioscience Biotechnology and Biochemistry, 2006. **70**(10): p. 2335-2348.
10. Szymanski, W., et al., *A simple enantioconvergent and chemoenzymatic synthesis of optically active alpha-substituted amides.* Angew Chem Int Ed Engl, 2011. **50**(45): p. 10712-5.
11. Bidmanova, S., et al., *Development of an enzymatic fiber-optic biosensor for detection of halogenated hydrocarbons.* Anal Bioanal Chem, 2010. **398**(5): p. 1891-8.
12. Janssen, D.B., et al., *Cloning of 1,2-Dichloroethane Degradation Genes of Xanthobacter-Autotrophicus Gj10 and Expression and Sequencing of the Dhla Gene.* Journal of Bacteriology, 1989. **171**(12): p. 6791-6799.
13. Jesenska, A., et al., *Cloning, biochemical properties, and distribution of mycobacterial haloalkane dehalogenases.* Applied and Environmental Microbiology, 2005. **71**(11): p. 6736-6745.
14. Sato, Y., et al., *Two rhizobial strains, Mesorhizobium loti MAFF303099 and Bradyrhizobium japonicum, USDA110, encode haloalkane dehalogenases with novel structures and substrate specificities.* Applied and Environmental Microbiology, 2005. **71**(8): p. 4372-4379.

15. Hasan, K., et al., *Biochemical characteristics of the novel haloalkane dehalogenase DatA, isolated from the plant pathogen Agrobacterium tumefaciens C58.* Appl Environ Microbiol, 2011. **77**(5): p. 1881-4.
16. Fortova, A., et al., *DspA from Strongylocentrotus purpuratus: The first biochemically characterized haloalkane dehalogenase of non-microbial origin.* Biochimie, 2013. **95**(11): p. 2091-6.
17. Franken, S.M., et al., *Crystal-Structure of Haloalkane Dehalogenase - an Enzyme to Detoxify Halogenated Alkanes.* Embo Journal, 1991. **10**(6): p. 1297-1302.
18. Newman, J., et al., *Haloalkane dehalogenases: Structure of a Rhodococcus enzyme.* Biochemistry, 1999. **38**(49): p. 16105-16114.
19. Marek, J., et al., *Crystal structure of the haloalkane dehalogenase from Sphingomonas paucimobilis UT26.* Biochemistry, 2000. **39**(46): p. 14082-6.
20. Mazumdar, P.A., et al., *X-ray crystal structure of Mycobacterium tuberculosis haloalkane dehalogenase Rv2579.* Biochim Biophys Acta, 2008. **1784**(2): p. 351-62.
21. Chaloupkova, R., et al., *Structural and functional analysis of a novel haloalkane dehalogenase with two halide-binding sites.* Acta Crystallogr D Biol Crystallogr, 2014. **70**(Pt 7): p. 1884-97.
22. Jesenska, A., et al., *Biochemical characterization of haloalkane dehalogenases DrbA and DmbC, Representatives of a Novel Subfamily.* Appl Environ Microbiol, 2009. **75**(15): p. 5157-60.
23. Pavlova, M., et al., *The identification of catalytic pentad in the haloalkane dehalogenase DhmA from Mycobacterium avium N85: Reaction mechanism and molecular evolution.* Journal of Structural Biology, 2007. **157**(2): p. 384-392.
24. Hesseler, M., et al., *Cloning, functional expression, biochemical characterization, and structural analysis of a haloalkane dehalogenase from Plesiocystis pacifica SIR-1.* Appl Microbiol Biotechnol, 2011. **91**(4): p. 1049-60.
25. Gehret, J.J., et al., *Structure and activity of DmmA, a marine haloalkane dehalogenase.* Protein Science, 2012. **21**(2): p. 239-248.
26. Drienovska, I., et al., *Biochemical Characterization of a Novel Haloalkane Dehalogenase from a Cold-Adapted Bacterium.* Applied and Environmental Microbiology, 2012. **78**(14): p. 4995-4998.
27. Ollis, D.L., et al., *The Alpha/Beta-Hydrolase Fold.* Protein Engineering, 1992. **5**(3): p. 197-211.
28. Nardini, M. and B.W. Dijkstra, *alpha/beta hydrolase fold enzymes: the family keeps growing.* Current Opinion in Structural Biology, 1999. **9**(6): p. 732-737.
29. Holmquist, M., *Alpha/Beta-hydrolase fold enzymes: structures, functions and mechanisms.* Curr Protein Pept Sci, 2000. **1**(2): p. 209-35.

30. Otyepka, M. and J. Damborsky, *Functionally relevant motions of haloalkane dehalogenases occur in the specificity-modulating cap domains.* Protein Science, 2002. **11**(5): p. 1206-1217.
31. Pries, F., et al., *The Role of Spontaneous Cap Domain Mutations in Haloalkane Dehalogenase Specificity and Evolution.* Journal of Biological Chemistry, 1994. **269**(26): p. 17490-17494.
32. Damborsky, J. and J. Koca, *Analysis of the reaction mechanism and substrate specificity of haloalkane dehalogenases by sequential and structural comparisons.* Protein Engineering, 1999. **12**(11): p. 989-998.
33. Chovancova, E., et al., *Phylogenetic analysis of haloalkane dehalogenases.* Proteins-Structure Function and Bioinformatics, 2007. **67**(2): p. 305-316.
34. Bohac, M., et al., *Halide-stabilizing residues of haloalkane dehalogenases studied by quantum mechanic calculations and site-directed mutagenesis.* Biochemistry, 2002. **41**(48): p. 14272-14280.
35. Prokop, Z., et al., *Catalytic mechanism of the haloalkane dehalogenase LinB from Sphingomonas paucimobilis UT26.* Journal of Biological Chemistry, 2003. **278**(46): p. 45094-45100.
36. Janssen, D.B., *Evolving haloalkane dehalogenases.* Current Opinion in Chemical Biology, 2004. **8**(2): p. 150-159.
37. Verschueren, K.H.G., et al., *Crystallographic Analysis of the Catalytic Mechanism of Haloalkane Dehalogenase.* Nature, 1993. **363**(6431): p. 693-698.
38. Bosma, T., et al., *Steady-state and pre-steady-state kinetic analysis of halopropane conversion by a Rhodococcus haloalkane dehalogenase.* Biochemistry, 2003. **42**(26): p. 8047-8053.
39. Schanstra, J.P. and D.B. Janssen, *Kinetics of halide release of haloalkane dehalogenase: Evidence for a slow conformational change.* Biochemistry, 1996. **35**(18): p. 5624-5632.
40. Pavlova, M., et al., *Redesigning dehalogenase access tunnels as a strategy for degrading an anthropogenic substrate.* Nature Chemical Biology, 2009. **5**(10): p. 727-733.
41. Damborsky, J., et al., *Structure-specificity relationships for haloalkane dehalogenases.* Environmental Toxicology and Chemistry, 2001. **20**(12): p. 2681-2689.
42. Koudelakova, T., et al., *Substrate specificity of haloalkane dehalogenases.* Biochemical Journal, 2011. **435**: p. 345-354.
43. Klvana, M., et al., *Pathways and Mechanisms for Product Release in the Engineered Haloalkane Dehalogenases Explored Using Classical and Random Acceleration Molecular Dynamics Simulations.* Journal of Molecular Biology, 2009. **392**(5): p. 1339-1356.
44. Ota, N. and D.A. Agard, *Enzyme specificity under dynamic control II: Principal component analysis of alpha-lytic protease using global and*

local solvent boundary conditions. Protein Science, 2001. **10**(7): p. 1403-1414.
45. Westerbeek, A., et al., *Dynamic Kinetic Resolution Process Employing Haloalkane Dehalogenase.* Acs Catalysis, 2011. **1**(12): p. 1654-1660.
46. Pieters, R.J., et al., *The enantioselectivity of haloalkane dehalogenases.* Tetrahedron Letters, 2001. **42**(3): p. 469-471.
47. Straathof, A.J.J. and J.A. Jongejan, *The enantiomeric ratio: origin, determination and prediction.* Enzyme and Microbial Technology, 1997. **21**(8): p. 559-571.
48. Bosma, T., et al., *Utilization of trihalogenated propanes by Agrobacterium radiobacter AD1 through heterologous expression of the haloalkane dehalogenase from Rhodococcus sp strain m15-3.* Applied and Environmental Microbiology, 1999. **65**(10): p. 4575-4581.
49. Lahoda, M., et al., *Crystallographic analysis of 1,2,3-trichloropropane biodegradation by the haloalkane dehalogenase DhaA31.* Acta Crystallographica Section D-Biological Crystallography, 2014. **70**: p. 209-217.
50. Holloway, P., et al., *Alteration of the substrate range of haloalkane dehalogenase by site-directed mutagenesis.* Biotechnology and Bioengineering, 1998. **59**(4): p. 520-523.
51. Biedermannova, L., et al., *A Single Mutation in a Tunnel to the Active Site Changes the Mechanism and Kinetics of Product Release in Haloalkane Dehalogenase LinB.* Journal of Biological Chemistry, 2012. **287**(34): p. 29062-29074.
52. Droge, M.J., et al., *Directed evolution of Bacillus subtilis lipase A by use of enantiomeric phosphonate inhibitors: Crystal structures and phage display selection.* Chembiochem, 2006. **7**(1): p. 149-157.
53. Nagata, Y., et al., *Purification and Characterization of Gamma-Hexachlorocyclohexane (Gamma-Hch) Dehydrochlorinase (Lina) from Pseudomonas-Paucimobilis.* Bioscience Biotechnology and Biochemistry, 1993. **57**(9): p. 1582-1583.
54. Nagasawa, S., et al., *Aerobic Mineralization of Gamma-Hch by Pseudomonas-Paucimobilis Ut26.* Chemosphere, 1993. **26**(9): p. 1719-1728.
55. Hynkova, K., et al., *Identification of the catalytic triad in the haloalkane dehalogenase from Sphingomonas paucimobilis UT26.* Febs Letters, 1999. **446**(1): p. 177-181.
56. Oakley, A.J., et al., *Crystal structure of haloalkane dehalogenase LinB from Sphingomonas paucimobilis UT26 at 0.95 angstrom resolution: Dynamics of catalytic residues.* Biochemistry, 2004. **43**(4): p. 870-878.
57. Chaloupkova, R., et al., *Modification of activity and specificity of haloalkane dehalogenase from Sphingomonas paucimobilis UT26 by engineering of its entrance tunnel.* Journal of Biological Chemistry, 2003. **278**(52): p. 52622-52628.

58. Stock, A.M., V.L. Robinson, and P.N. Goudreau, *Two-component signal transduction.* Annual Review of Biochemistry, 2000. **69**: p. 183-215.
59. Hess, J.F., et al., *Protein-Phosphorylation and Bacterial Chemotaxis.* Cold Spring Harbor Symposia on Quantitative Biology, 1988. **53**: p. 41-48.
60. Mizuno, T., *His-Asp phosphotransfer signal transduction.* Journal of Biochemistry, 1998. **123**(4): p. 555-563.
61. Nixon, B.T., C.W. Ronson, and F.M. Ausubel, *2-Component Regulatory Systems Responsive to Environmental Stimuli Share Strongly Conserved Domains with the Nitrogen Assimilation Regulatory Genes Ntrb and Ntrc.* Proceedings of the National Academy of Sciences of the United States of America, 1986. **83**(20): p. 7850-7854.
62. Urao, T., et al., *A transmembrane hybrid-type histidine kinase in arabidopsis functions as an osmosensor.* Plant Cell, 1999. **11**(9): p. 1743-1754.
63. Nishimura, C., et al., *Histidine kinase homologs that act as cytokinin receptors possess overlapping functions in the regulation of shoot and root growth in Arabidopsis.* Plant Cell, 2004. **16**(6): p. 1365-1377.
64. Deng, Y., et al., *Arabidopsis Histidine Kinase CKI1 Acts Upstream of HISTIDINE PHOSPHOTRANSFER PROTEINS to Regulate Female Gametophyte Development and Vegetative Growth.* Plant Cell, 2010. **22**(4): p. 1232-1248.
65. Horak, J., et al., *Molecular Mechanisms of Signalling Specificity Via Phosphorelay Pathways in Arabidopsis.* Current Protein & Peptide Science, 2011. **12**(2): p. 126-136.
66. Pischke, M.S., et al., *An Arabidopsis histidine kinase is essential for megagametogenesis.* Proceedings of the National Academy of Sciences of the United States of America, 2002. **99**(24): p. 15800-15805.
67. Urao, T., K. Yamaguchi-Shinozaki, and K. Shinozaki, *Two-component systems in plant signal transduction.* Trends in Plant Science, 2000. **5**(2): p. 67-74.
68. Hwang, D., H.C. Chen, and J. Sheen, *Two-component signal transduction pathways in Arabidopsis.* Plant Physiology, 2002. **129**(2): p. 500-515.
69. Grefen, C. and K. Harter, *Plant two-component systems: principles, functions, complexity and cross talk.* Planta, 2004. **219**(5): p. 733-742.
70. Ueguchi, C., et al., *Novel family of sensor histidine kinase genes in Arabidopsis thaliana.* Plant and Cell Physiology, 2001. **42**(2): p. 231-235.
71. Davies, P., *The Plant Hormones: Their Nature, Occurrence, and Functions*, in *Plant Hormones*, P. Davies, Editor. 1995, Springer Netherlands. p. 1-12.

72. West, A.H. and A.M. Stock, *Histidine kinases and response regulator proteins in two-component signaling systems.* Trends in Biochemical Sciences, 2001. **26**(6): p. 369-376.
73. Heyl, A. and T. Schmulling, *Cytokinin signal perception and transduction.* Current Opinion in Plant Biology, 2003. **6**(5): p. 480-488.
74. Ferreira, F.J. and J.J. Kieber, *Cytokinin signaling.* Current Opinion in Plant Biology, 2005. **8**(5): p. 518-525.
75. Hothorn, M., T. Dabi, and J. Chory, *Structural basis for cytokinin recognition by Arabidopsis thaliana histidine kinase 4.* Nature Chemical Biology, 2011. **7**(11): p. 766-768.
76. Lomin, S.N., et al., *Receptor Properties and Features of Cytokinin Signaling.* Acta Naturae, 2012. **4**(3): p. 31-45.
77. Yamada, H., et al., *The Arabidopsis AHK4 histidine kinase is a cytokinin-binding receptor that transduces cytokinin signals across the membrane.* Plant and Cell Physiology, 2001. **42**(9): p. 1017-1023.
78. Kakimoto, T., *CKI1, a histidine kinase homolog implicated in cytokinin signal transduction.* Science, 1996. **274**(5289): p. 982-985.
79. Hwang, I. and J. Sheen, *Two-component circuitry in Arabidopsis cytokinin signal transduction.* Nature, 2001. **413**(6854): p. 383-389.
80. Hejatko, J., et al., *The putative sensor histidine kinase CKI1 is involved in female gametophyte development in Arabidopsis.* Molecular Genetics and Genomics, 2003. **269**(4): p. 443-453.
81. Pekarova, B., et al., *Structure and binding specificity of the receiver domain of sensor histidine kinase CKI1 from Arabidopsis thaliana.* Plant Journal, 2011. **67**(5): p. 827-839.
82. Desikan, R., et al., *The Histidine Kinase AHK5 Integrates Endogenous and Environmental Signals in Arabidopsis Guard Cells.* Plos One, 2008. **3**(6).
83. Bleecker, A.B., et al., *The ethylene-receptor family from Arabidopsis: structure and function.* Philosophical Transactions of the Royal Society of London Series B-Biological Sciences, 1998. **353**(1374): p. 1405-1412.
84. Schaller, G.E., et al., *The Ethylene Response Mediator Etr1 from Arabidopsis Forms a Disulfide-Linked Dimer.* Journal of Biological Chemistry, 1995. **270**(21): p. 12526-12530.
85. Hall, A.E., et al., *Ethylene perception by the ERS1 protein in Arabidopsis.* Plant Physiology, 2000. **123**(4): p. 1449-1457.
86. Guo, H.W. and J.R. Ecker, *The ethylene signaling pathway: new insights.* Current Opinion in Plant Biology, 2004. **7**(1): p. 40-49.
87. Aravind, L. and C.P. Ponting, *The GAF domain: an evolutionary link between diverse phototransducing proteins.* Trends in Biochemical Sciences, 1997. **22**(12): p. 458-459.
88. Martinez, S.E., et al., *The two GAF domains in phosphodiesterase 2A have distinct roles in dimerization and in cGMP binding.* Proceedings of

the National Academy of Sciences of the United States of America, 2002. **99**(20): p. 13260-13265.
89. Gao, Z., et al., *Heteromeric interactions among ethylene receptors mediate signaling in Arabidopsis.* Journal of Biological Chemistry, 2008. **283**(35): p. 23801-23810.
90. Muller-Dieckmann, H.J., A.A. Grantz, and S.H. Kim, *The structure of the signal receiver domain of the Arabidopsis thaliana ethylene receptor ETR1.* Structure with Folding & Design, 1999. **7**(12): p. 1547-1556.
91. Xu, Q.P. and A.H. West, *Conservation of structure and function among histidine-containing phosphotransfer (HPt) domains as revealed by the crystal structure of YPD1.* Journal of Molecular Biology, 1999. **292**(5): p. 1039-1050.
92. Wohlbach, D.J., B.F. Quirino, and M.R. Sussman, *Analysis of the Arabidopsis histidine kinase ATHK1 reveals a connection between vegetative osmotic stress sensing and seed maturation.* Plant Cell, 2008. **20**(4): p. 1101-1117.
93. Punwani, J.A., et al., *The subcellular distribution of the Arabidopsis histidine phosphotransfer proteins is independent of cytokinin signaling.* Plant Journal, 2010. **62**(3): p. 473-482.
94. Suzuki, T., et al., *An Arabidopsis histidine-containing phosphotransfer (HPt) factor implicated in phosphorelay signal transduction: Overexpression of AHP2 in plants results in hypersensitiveness to cytokinin.* Plant and Cell Physiology, 2002. **43**(1): p. 123-129.
95. Hutchison, C.E., et al., *The Arabidopsis histidine phosphotransfer proteins are redundant positive regulators of cytokinin signaling.* Plant Cell, 2006. **18**(11): p. 3073-3087.
96. Mahonen, A.P., et al., *Cytokinin signaling and its inhibitor AHP6 regulate cell fate during vascular development.* Science, 2006. **311**(5757): p. 94-98.
97. Jung, K.W., et al., *Arabidopsis histidine-containing phosphotransfer factor 4 (AHP4) negatively regulates secondary wall thickening of the anther endothecium during flowering.* Molecules and Cells, 2008. **25**(2): p. 294-300.
98. Kato, M., et al., *Refined structure of the histidine-containing phosphotransfer (HPt) domain of the anaerobic sensor kinase ArcB from Escherichia coli at 1.57 angstrom resolution.* Acta Crystallographica Section D-Biological Crystallography, 1999. **55**: p. 1842-1849.
99. Mourey, L., et al., *Crystal structure of the CheA histidine phosphotransfer domain that mediates response regulator phosphorylation in bacterial chemotaxis.* Journal of Biological Chemistry, 2001. **276**(33): p. 31074-31082.

100. Xu, Q.P., et al., *Crystal Structure of Histidine Phosphotransfer Protein ShpA, an Essential Regulator of Stalk Biogenesis in Caulobacter crescentus.* Journal of Molecular Biology, 2009. **390**(4): p. 686-698.
101. Sugawara, H., et al., *Crystal structure of the histidine-containing phosphotransfer protein ZmHP2 from maize.* Protein Science, 2005. **14**(1): p. 202-208.
102. Levin, E.J., et al., *Ensemble refinement of protein crystal structures: Validation and application.* Structure, 2007. **15**(9): p. 1040-1052.
103. Ruszkowski, M., et al., *Medicago truncatula histidine-containing phosphotransfer protein Structural and biochemical insights into the cytokinin transduction pathway in plants.* Febs Journal, 2013. **280**(15): p. 3709-3720.
104. Bauer, J., et al., *Structure-Function Analysis of Arabidopsis thaliana Histidine Kinase AHK5 Bound to Its Cognate Phosphotransfer Protein AHP1.* Molecular Plant, 2013. **6**(3): p. 959-970.
105. Degtjarik, O., et al., *Cloning, expression, purification, crystallization and preliminary X-ray diffraction analysis of AHP2, a signal transmitter protein from Arabidopsis thaliana.* Acta Crystallographica Section F-Structural Biology and Crystallization Communications, 2013. **69**: p. 158-161.
106. Imamura, A., et al., *Response regulators implicated in His-to-Asp phosphotransfer signaling in Arabidopsis.* Proceedings of the National Academy of Sciences of the United States of America, 1998. **95**(5): p. 2691-2696.
107. Sakai, H., et al., *Two-component response regulators from Arabidopsis thaliana contain a putative DNA-binding motif.* Plant and Cell Physiology, 1998. **39**(11): p. 1232-1239.
108. Imamura, A., et al., *Compilation and characterization of Arabidopsis thaliana response regulators implicated in His-Asp phosphorelay signal transduction.* Plant and Cell Physiology, 1999. **40**(7): p. 733-742.
109. Schaller, G.E., et al., *Nomenclature for two-component signaling elements of rice.* Plant Physiology, 2007. **143**(2): p. 555-557.
110. Makino, S., et al., *Genes encoding pseudo-response regulators: Insight into His-to-Asp phosphorelay and circadian rhythm in Arabidopsis thaliana.* Plant and Cell Physiology, 2000. **41**(6): p. 791-803.
111. Matsushika, A., et al., *Circadian waves of expression of the APRR1/TOC1 family of pseudo-response regulators in Arabidopsis thaliana: Insight into the plant circadian clock.* Plant and Cell Physiology, 2000. **41**(9): p. 1002-1012.
112. Nakamichi, N., et al., *The Arabidopsis pseudo-response regulators, PRR5 and PRR7, coordinately play essential roles for circadian clock function.* Plant and Cell Physiology, 2005. **46**(4): p. 609-619.

113. To, J.P.C., et al., *Type-A Arabidopsis response regulators are partially redundant negative regulators of cytokinin signaling.* Plant Cell, 2004. **16**(3): p. 658-671.
114. Lohrmann, J. and K. Harter, *Plant two-component signaling systems and the role of response regulators.* Plant Physiology, 2002. **128**(2): p. 363-369.
115. Argueso, C.T., et al., *Two-Component Elements Mediate Interactions between Cytokinin and Salicylic Acid in Plant Immunity.* Plos Genetics, 2012. **8**(1).
116. Jeon, J., et al., *A Subset of Cytokinin Two-component Signaling System Plays a Role in Cold Temperature Stress Response in Arabidopsis.* Journal of Biological Chemistry, 2010. **285**(30): p. 23369-23384.
117. Imamura, A., Y. Yoshino, and T. Mizuno, *Cellular localization of the signaling components of Arabidopsis His-to-Asp phosphorelay.* Bioscience Biotechnology and Biochemistry, 2001. **65**(9): p. 2113-2117.
118. Hosoda, K., et al., *Molecular structure of the GARP family of plant Myb-related DNA binding motifs of the Arabidopsis response regulators.* Plant Cell, 2002. **14**(9): p. 2015-2029.
119. Sakai, H., T. Aoyama, and A. Oka, *Arabidopsis ARR1 and ARR2 response regulators operate as transcriptional activators.* Plant Journal, 2000. **24**(6): p. 703-711.
120. Kiba, T., et al., *Characterization of a novel type response regulator, ARR22, implicated in His-to-Asp phosphorelay signal transduction in A-thaliana.* Plant and Cell Physiology, 2004. **45**: p. S41-S41.
121. Gattolin, S., et al., *Spatial and temporal expression of the response regulators ARR22 and ARR24 in Arabidopsis thaliana.* Journal of Experimental Botany, 2006. **57**(15): p. 4225-4233.
122. Kiba, T., et al., *Combinatorial microarray analysis revealing Arabidopsis genes implicated in cytokinin responses through the His -> Asp phosphorelay circuitry.* Plant and Cell Physiology, 2005. **46**(2): p. 339-355.
123. Dortay, H., et al., *Analysis of protein interactions within the cytokinin-signaling pathway of Arabidopsis thaliana.* Febs Journal, 2006. **273**(20): p. 4631-4644.
124. Nakamura, A., et al., *Biochemical characterization of a putative cytokinin-responsive his-kinase, CKI1, from Arabidopsis thaliana.* Bioscience Biotechnology and Biochemistry, 1999. **63**(9): p. 1627-1630.
125. Scharein, B., et al., *Ethylene signaling: Identification of a putative ETR1-AHP1 phosphorelay complex by fluorescence spectroscopy.* Analytical Biochemistry, 2008. **377**(1): p. 72-76.

126. Scharein, B. and G. Groth, *Phosphorylation Alters the Interaction of the Arabidopsis Phosphotransfer Protein AHP1 with Its Sensor Kinase ETR1*. Plos One, 2011. **6**(9).
127. Rupp, B., *Biomolecular Crystallography: Principles, Practice, and Application to Structural Biology*. 2010: Garland Science.
128. Chayen, N.E. and E. Saridakis, *Protein crystallization: from purified protein to diffraction-quality crystal.* Nature Methods, 2008. **5**(2): p. 147-153.
129. McPherson, A., *Crystallization of Biological Macromolecules*. 1999: Cold Spring Harbor Laboratory Press.
130. Chayen, N.E., *Turning protein crystallisation from an art into a science.* Current Opinion in Structural Biology, 2004. **14**(5): p. 577-583.
131. Asherie, N., *Protein crystallization and phase diagrams.* Methods, 2004. **34**(3): p. 266-272.
132. Chayen, N.E., *Methods for separating nucleation and growth in protein crystallisation.* Progress in Biophysics & Molecular Biology, 2005. **88**(3): p. 329-337.
133. Luft, J.R., J. Newman, and E.H. Snell, *Crystallization screening: the influence of history on current practice.* Acta Crystallographica Section F-Structural Biology Communications, 2014. **70**: p. 835-853.
134. Snell, E.H., et al., *The application and use of chemical space mapping to interpret crystallization screening results.* Acta Crystallographica Section D-Biological Crystallography, 2008. **64**: p. 1240-1249.
135. Bergfors, T.M., *Protein Crystallization*. IUL biotechnology series. 2009: International University Line.
136. Chayen, N.E., P.D.S. Stewart, and D.M. Blow, *Microbatch Crystallization under Oil - a New Technique Allowing Many Small-Volume Crystallization Trials.* Journal of Crystal Growth, 1992. **122**(1-4): p. 176-180.
137. Ng, J.D., J.A. Gavira, and J.M. Garcia-Ruiz, *Protein crystallization by capillary counterdiffusion for applied crystallographic structure determination.* Journal of Structural Biology, 2003. **142**(1): p. 218-231.
138. Garcia-Ruiz, J.M., et al., *Teaching protein crystallisation by the gel acupuncture method.* Journal of Chemical Education, 1998. **75**(4): p. 442-446.
139. Trakhanov, S. and F.A. Quiocho, *Influence of Divalent-Cations in Protein Crystallization.* Protein Science, 1995. **4**(9): p. 1914-1919.
140. Mcpherson, A., et al., *The Effects of Neutral Detergents on the Crystallization of Soluble-Proteins.* Journal of Crystal Growth, 1986. **76**(3): p. 547-553.
141. Mcpherson, A., *Current Approaches to Macromolecular Crystallization.* European Journal of Biochemistry, 1990. **189**(1): p. 1-23.

142. Bergfors, T., *Seeds to crystals.* Journal of Structural Biology, 2003. **142**(1): p. 66-76.
143. Rhodes, G., *Crystallography Made Crystal Clear: A Guide for Users of Macromolecular Models*. Complementary Science. 2010: Elsevier Science.
144. Jan, D., *Principles of Protein X-ray Crystallography*. Springer advanced texts in chemistry. 1999: Springer.
145. Faust, A., et al., *A tutorial for learning and teaching macromolecular crystallography.* Journal of Applied Crystallography, 2008. **41**: p. 1161-1172.
146. Taylor, G., *The phase problem.* Acta Crystallographica Section D-Biological Crystallography, 2003. **59**: p. 1881-1890.
147. Faust, A., et al., *Update on the tutorial for learning and teaching macromolecular crystallography.* Journal of Applied Crystallography, 2010. **43**: p. 1230-1237.
148. Ravelli, R.B.G., et al., *Phasing in the presence of radiation damage.* Journal of Synchrotron Radiation, 2005. **12**: p. 276-284.
149. Nanao, M.H., G.M. Sheldrick, and R.B.G. Ravelli, *Improving radiation-damage substructures for RIP.* Acta Crystallographica Section D-Biological Crystallography, 2005. **61**: p. 1227-1237.
150. Petrek, M., et al., *CAVER: a new tool to explore routes from protein clefts, pockets and cavities.* Bmc Bioinformatics, 2006. **7**.
151. Diederichs, K. and P.A. Karplus, *Improved R-factors for diffraction data analysis in macromolecular crystallography.* Nat Struct Biol, 1997. **4**(4): p. 269-75.
152. Weiss, M.S. and R. Hilgenfeld, *On the use of the merging R factor as a quality indicator for X-ray data.* Journal of Applied Crystallography, 1997. **30**: p. 203-205.
153. Bradford, M.M., *A rapid and sensitive method for the quantitation of microgram quantities of protein utilizing the principle of protein-dye binding.* Anal Biochem, 1976. **72**: p. 248-54.
154. Streltsov, V.A., et al., *Haloalkane dehalogenase LinB from Sphingomonas paucimobilis UT26: X-ray crystallographic studies of dehalogenation of brominated substrates.* Biochemistry, 2003. **42**(34): p. 10104-10112.
155. Smatanova, I., et al., *Crystallization and preliminary X-ray diffraction analysis of haloalkane dehalogenase LinB from Sphingomonas paucimobilis UT26.* Acta Crystallographica Section D-Biological Crystallography, 1999. **55**: p. 1231-1233.